IMPACT ASSESSMENT OF CLIMATE CHANGE ON HYDROLOGICAL REGIME IN SABARI SUB-BASIN GODAVARI RIVER SYSTEM

NATIONAL INSTITUTE OF HYDROLOGY,
JAL VIGYAN BHAVAN
ROORKEE – 247 667 (UTTARANCHAL)

2009 - 2013

PREFACE

Climate change is not only a major global environmental problem, but also an issue of great concern to a developing country like India. India needs to be much more concerned since its vast population largely depends on climate sensitive sectors like agriculture, forestry and fishery for livelihood. Climate change could represent additional stress on the ecological and socio-economic systems that are already facing tremendous pressure due to rapid industrialization, urbanization and economic development. With climate change, there would be increasing scarcity of water, reduction in yields of forest biomass, and increased risk to human health. India released its National Action Plan on Climate Change (NAPCC) in June, 2008 to outline its strategy to meet the Climate Change challenge. The National Action Plan stresses to maintain a high growth rate which is essential for increasing the living standards of the vast majority of people of India but at the same time reduce their vulnerability to the climate change impacts. The National Action Plan identifies measures that promote the objectives of sustainable development while also yielding the benefits for addressing climate change. Eight National Missions under the National Action Plan, represents a multi-pronged, long term and integrated strategies for achieving key goals in the context of climate change.

In this report the trend analyses of climatic variables (rainfall & temperature) were carried out for Sabari sub-basin Godavari River System using historical period of 109 years (1901 to 2009). Mann-Kendall trend analysis was used to predict the trends of the climatic variables in the study area. The daily rainfall-runoff modeling was carried out using ARNO model for a period of 39 years (1970 to 2008). Calibration and validation was carried out for a period of 30 years (1970 to 1999) and 9 (2000 to 2008) years respectively. The runoff was predicted using the IMD (Indian Meteorological Department) and RCM (Regional Circulation Model) downscaled data for the base line period (1960-1990), Mid (2021 to 2050) and End Century (2071 to 2098) periods.

This report was prepared by Dr.V.S.Jeyakanthan, Sc-D, Dr.Y.R.Satyaji Rao, Sc-F and B.Krishna, Sc-C of Deltaic Regional Centre of the Institute.

(Raj Dev Singh)
Director

CONTENTS Page No.

ABSTRACT i

CHAPTER-1: INTRODUCTION 1
1.0 Impact of climate change on hydrological regime 2
1.1 Precipitation 2
1.2 Runoff 2
1.3 Floods and Droughts 3
1.4 Snow melt and Glaciers 3
1.5 Water Quality Issues 3
1.6 Water stress and food security 3
1.7 Water Management Issues 4
1.8 Objectives 4
CHAPTER-2: Literature Review 5
CHAPTER-3: Study Area 9
3.1 General 9
3.2 Agricultural 9
3.3 Rainfall 9
3.4 Temperature 11
3.5 Physiography 11
3.6 Soils 11
3.7 Mineral resources and forest
CHAPTER-4: METHODOLOGY 12
4.1 General 12
4.2 Representation of hydrological processes 12
4.3 Soil Moisture Balance Module 13
4.4 The Evapotranspiration Module 17
4.5 The ARNO model parameters 19
CHAPTER-5: RESULTS & DISCUSSION 21
5.1 Trend analysis of climatic variables (Rainfall and Temperature) of Sabari sub-basin using Mann-Kendall Test for the historical data 1901-2009 (109 years) 21
5.2 Rainfall-Runoff modeling of Sabari Sub-basin Using ARNO model 27
5.3.1 Analysis of RCM downscaled data 29
5.3.2 Analysis of RCM downscaled temperature data (Daily Max.Temp) for the Baseline (1961-1990), Mid Century (2021-2050) and End Century (2071-2098) periods 29
5.3.3 Analysis of RCM downscaled daily Rainfall data for the Baseline (1961-1990), MidCentury (2021-2050) and End Century (2071-2098) periods. 32
5.4 Impact of climate change in the study area for various hydrological Scenarios 34
CHAPTER-6: CONCLUSIONS 37
References 38

Abstract

Trend analyses of climatic variables (rainfall & temperature) were carried out for Sabari sub-basin using historical period of 109 years (1901 to 2009). Mann-Kendall trend analysis was used to predict the trends of the climatic variables in the study area. The results reveals that the temperature is in increasing trend in the all the months with 95% confidence level. Whereas, rainfall has no trend in monsoon period except the September month shows decreasing trend. Linear trend analysis were also carried out, the results of linear analysis also in line with Mann-Kendall outcome.

The daily rainfall-runoff modeling was carried out using ARNO model for a period of 39 years (1970 to 2008). Calibration and validation was carried out for a period of 30 years (1970 to 1999) and 9 (2000 to 2008) years respectively. The model efficiency during the calibration and validation run was 72.35% and 70.16% respectively. RCM downscaled data for base line (1960 to 1990), mid-century (2021 to 2050) and end-century (2071 to 2098) period obtained from IITM, Pune has been used in the validated ARNO model for the analysis of hydrological scenarios due to climate change in the sub-basin.

The IMD and RCM downscaled data for the base line period (1960-1990) has been compared and found that there is in huge variation in both the temperature and rainfall measurements. The minimum and maximum temperature measured by the IMD was 22.3 and 38.7 ^{o}C whereas predicted by RCM was 32.5 and 48.6 ^{o}C respectively. For the above said period the average temperature measured by IMD and predicted by RCM was 32.8 and 40.2 ^{o}C respectively. The RCM downscaled data shows that the minimum, maximum and average temperature predicted during the summer season for Mid Century period is 34.7, 50.6 and 43.5^{o}C respectively. The values for the End Century period is 35.8, 53.4 and 45.3 ^{o}C. The maximum rainfall measured by IMD and predicted by RCM for the base line period is 485.1 and 1235.47 mm respectively. Whereas for the Mid and End century period is 115.54 and 1237.25 mm respectively. The runoff predicted using the RCM data for the Mid (2021 to 2050) and End Century (2071 to 2098) periods show a frequent high peak floods like scenario.

CHAPTER-1
INTRODUCTION

Global warming induced by increased green house gas (GHG) emissions since last century is reported to have causing climate change on Earth. However, global climate change is actually much more complicated than that because a change in the temperature can cause changes in other weather elements. Climate varies from place to place, depending on latitude, distance to the sea, vegetation, orography and other factors. Similar to weather, the climate variability also occurs at different time and space scales. A long term prognostic projection of climate over a region is important and useful in developing coping strategies or mitigation measures.

Plants, animals, natural and managed ecosystems, and human settlements are susceptible to variations in the storage, fluxes, and quality of water. All of these, in turn, are sensitive to climate change. With robust scientific evidence showing that human-induced climate change is occurring, it is critical to understand how water quantity and quality might be affected. Effects of climate on the nation's water storage capabilities and hydrologic functions will have significant implications for water management and planning as variability in natural processes increases.

The intergovernmental panel on climate change (IPCC) assessment reports has brought out a number inferences based on modeling I simulation studies carried out on climate change scenarios. Following sections contain extracts from IPCC reports relevant to hydrology and water resources:

Projected Change in Climate

Best-estimate projections from models indicate that decadal average warming over each inhabited continent by 2030 is very likely to be at least twice as large (around 0.2°C per decade) as the corresponding model-estimated natural variability during the 20th century. Continued greenhouse gas emissions at or above current rates would cause further warming and induce many changes in the global climate system during the 21st century, with these changes very likely to be larger than those observed during the 20th century. Projected global average temperature change for 2090-2099 (relative to 1980-1999), ranges from 1.8°C to 4.0°C.

Warming is projected to be greatest over land and at most high northern latitudes, and least over the Southern Ocean and parts of the North Atlantic Ocean. It is very likely that hot extremes and heat waves will continue to become more frequent. Uncertainties in projected changes in the hydrological system arise from internal variability of the climate system.

1.0 IMPACT OF CLIMATE CHANGE ON HYDROLOGICAL REGIME

The prediction envisages: Increasing atmospheric water vapour content; changing precipitation patterns, intensity and extremes; reduced snow cover and widespread melting of ice; and changes in soil moisture and runoff. Precipitation changes show substantial spatial and inter-decadal variability. Over the 20th century, precipitation has mostly increased over land in high northern latitudes, while decreases have dominated in the tropics and subtropics since 1970.

1.1 Precipitation

The frequency of heavy precipitation events (or proportion of total rainfall from heavy falls) has increased over most areas. Globally, the area of land classified as very dry has more than doubled since the 1970s. There have been significant decreases in water storage in mountain glaciers and Northern Hemisphere snow cover. Shifts in the amplitude and timing of runoff in glacier- and snowmelt-fed rivers, and in ice related phenomena in rivers and lakes, have been observed. Climate model simulations for the 21 st century are consistent in projecting precipitation increases in high latitudes and parts of the tropics, and decreases in some subtropical and lower mid-latitude regions. Outside these areas, the sign and magnitude of projected changes varies.

1.2 Runoff

By the middle of the 21st century, annual average river runoff and water availability are projected to increase as a result of climate change at high latitudes and in some wet tropical areas, and decrease over some dry regions at mid-latitudes and in the dry tropics. Many semi-arid and arid areas (e.g., the Mediterranean Basin, western USA, southern Africa and northeastern

Brazil) are particularly exposed to the impacts of climate change and are projected to suffer a decrease of water resources due to climate change.

1.3 Floods and Droughts

Increased precipitation intensity and variability are projected to increase the risks of flooding and drought in many areas. The frequency of heavy precipitation events (or proportion of total rainfall from heavy falls) will be very likely to increase over most areas during the 21st century, with consequences for the risk of rain-generated floods. At the same time, the proportion of land surface in extreme drought at any one time is projected to increase, in addition to a tendency for drying in continental interiors during summer, especially in the sub-tropics, low and mid-latitudes.

1.4 Snow melt and Glaciers

Water supplies stored in glaciers and snow cover are projected to decline in the course of the century, thus reducing water availability during warm and dry periods (through a seasonal shift in streamflow, an increase in the ratio of winter to annual flows, and reductions in low flows) in regions supplied by melt water from major mountain ranges, where more than one-sixth of the world's population currently live.

1.5 Water Quality Issues

Higher water temperatures and changes in extremes, including floods and droughts, are projected to affect water quality and exacerbate many forms of water pollution from sediments, nutrients, dissolved organic carbon, pathogens, pesticides and salt, as well as thermal pollution, with possible negative impacts on ecosystems, human health, and water system reliability and operating costs. In addition, sea-level rise is projected to extend areas of salinisation of groundwater and estuaries, resulting in a decrease of freshwater availability for humans and ecosystems in coastal areas.

1.6 Water stress and food security

Globally, the negative impacts of future climate change on freshwater systems are expected to outweigh the benefits. By the 2050s, the area of land subject to increasing water stress due to climate change is projected to be more than double that with decreasing water stress. Areas in which runoff is projected to decline face a clear reduction in the value of the services provided

by water resources. Increased annual runoff in some areas is projected to lead to increased total water supply.

However, in many regions, this benefit is likely to be counterbalanced by the negative effects of increased precipitation variability and seasonal runoff shifts in water supply, water quality and flood risks. Changes in water quantity and quality due to climate change are expected to affect food availability, stability, access and utilisation. This is expected to lead to decreased food security and increased vulnerability of poor rural farmers, especially in the arid and semi-arid tropics and Asian and African mega deltas.

1.7 Water Management Issues

Climate change affects the function and operation of existing water infrastructure including hydropower, structural flood defences, drainage and irrigation systems - as well as water management practices. Adverse effects of climate change on freshwater systems aggravate the impacts of other stresses, such as population growth, changing economic activity, land-use change and urbanisation. Globally, water demand will grow in the coming decades, primarily due to population growth and increasing affluence; regionally, large changes in irrigation water demand as a result of climate change are expected. Current water management practices may not be robust enough to cope with the impacts of climate change on water supply reliability, flood risk, health, agriculture, energy and aquatic ecosystems. In many locations, water management cannot satisfactorily cope even with current climate variability, so that large flood and drought damages occur. As a first step, improved incorporation of information about current climate variability into water-related management would assist adaptation to longer-term climate change impacts. Climatic and non-climatic factors, such as growth of population and damage potential, would exacerbate problems in the future.

1.8 Objectives:

- Trend analysis of climatic variables (Rainfall and Temperature) of Sabari sub-basin using historical data1901-2009(109 years).
- Rainfall-runoff modeling of Sabari sub-basin using ARNO model.
- Development of various hydrological scenarios of the sub-basin using downscaled data.

Chapter-2

Literature Review

Historical trends in precipitation, temperature, and streamflows in the Great Lakes were examined by McBean and Motiee (2006) using regression analysis and Mann-Kendall statistics, the results emphasizes that many of these variables demonstrate statistically significant increases ongoing for a six decade period. Future precipitation rates as predicted using fitted regression lines were compared with scenarios from Global Climate Change Models (GCMs) and demonstrate similar forecast predictions for Lake Superior. Trend projections from historical data are, however, higher than GCM predictions for Michigan/Huron. Significant variability in predictions, as developed from alternative GCMs, is noted. Given the general agreement as derived from very different procedures, predictions extrapolated from historical trends and from GCMs, there is evidence that hydrologic changes in the Great Lakes Basin are likely the result of climate change.

Cannon and Hsieh (2008) has mentioned that robust variants of nonlinear canonical correlation analysis (NLCCA) are introduced to improve performance on datasets with low signal-to-noise ratios, for example those encountered when making seasonal climate forecasts. The neural network model architecture of standard NLCCA is kept intact, but the cost functions used to set the model parameters are replaced with more robust variants. The Pearson product-moment correlation in the double-barreled network is replaced by the biweight midcorrelation, and the mean squared error (mse) in the inverse mapping networks can be replaced by the mean absolute error (mae). Robust variants of NLCCA are demonstrated on a synthetic dataset and are used to forecast sea surface temperatures in the tropical Pacific Ocean based on the sea level pressure field. Results suggest that adoption of the biweight midcorrelation can lead to improved performance, especially when a strong, common event exists in both predictor/predictand datasets. Replacing the mse by the mae leads to improved performance on the synthetic dataset, but not on the climate dataset except at the longest lead time, which suggests that the appropriate cost function for the inverse mapping networks is more problem dependent

Droogers, Loon, and W. Immerzeel (2007) has explained that numerical simulation models are frequently applied to assess the impact of climate change on hydrology and agriculture. A common hypothesis is that unavoidable model errors are reflected in the reference situation as well as in the climate change situation so that 5 by comparing reference to scenario model errors will level out. For a polder in The Netherlands an innovative procedure has been introduced, referred to as the Model-Scenario-Ratio (MSR), to express model inaccuracy on climate change impact assessment. MSR values close to 1, indicating that impact assessment is mainly a function of the scenario itself rather than of the quality of the model, were found for 10 most indicators evaluated. More extreme climate change scenarios and indicators based on threshold values showed lower MSR values, indicating that model accuracy is an important component of the climate change impact assessment. It was concluded that the MSR approach can be applied easily and will lead to more robust impactassessment analyses

McBean and H. Motiee (2008) has given view 0f threshold of the appearance of global warming from theory to reality, extensive research has focused on predicting the impact of potential climate change on water resources using results from Global Circulation Models (GCMs). This research carries this further by statistical analyses of long term meteorological and hydrological data. Seventy years of historical trends in precipitation, temperature, and streamflows in the Great Lakes of North America are developed using long term regression analyses and Mann-Kendall statistics. The results generated by the two statistical procedures are in agreement and demonstrate that many of these variables are experiencing statistically significant increases over a seven-decade period. The trend lines of stream flows in the three rivers of St. Clair, Niagara and St. Lawrence, and precipitation levels over four of the five Great Lakes, show statistically significant increases in flows and precipitation. Further, precipitation rates as predicted using fitted regression lines are compared with scenarios from GCMs and demonstrate similar forecast predictions for Lake Superior. Trend projections from historical data are higher than GCM predictions for Lakes Michigan/Huron. Significant variability in predictions, as developed from alternative GCMs, is noted. Given the general agreement as derived from very different procedures, predictions extrapolated from historical trends and from GCMs, there is evidence that hydrologic changes particularly for the precipitation in the Great Lakes Basin may be demonstrating influences arising from global warming and climate change.

Chen;Wu and Qi Hu (2008) has given impacts of climate change on water resource in the Bosten Lake basin in the south slope of the Tianshan Mountains in Xinjiang, China, were evaluated using an artificial neural network model. The model was trained using the error backpropagation algorithm and validated for a major catchment that covers 82% of the Bosten Lake basin and has the only available weather and streamflow data. After validating the model it was used to examine the surface hydrology responses to changes of regional temperature and precipitation. Major results showed that because of an additional effect on glacier melt in the upper reach of the basin temperature increase can cause large increases of streamflow. Model results also showed that if the current climate trend continues, the annual streamflow would increase by 38% of its current volume, and the summer and winter streamflow would increase by 71.8 and 11.4% of their respective current volume in the next 50–70 years, highlighting challenges for the basin's water resources management and flood protection.

Fowler and Kilsby (2007) was explained that the daily rainfall and temperature data were extracted from the multi-ensemble HadRM3H regional climate model (RCM) integrations for control (1960–1990) and future (2070–2100) time-slices. This dynamically downscaled output was bias-corrected on observed mean statistics and used as input to hydrological models calibrated for eight catchments which are critical water resources in northwest England. Simulated daily flow distributions matched observed from Q_{95} to Q_5, suggesting that RCM data can be used with some confidence to examine future changes in flow regime. Under the SRES A2 (UKCIP02 Medium-High) scenario, annual runoff is projected to increase slightly at high elevation catchments, but reduce by 16% at lower elevations. Impacts on monthly flow distribution are significant, with summer reductions of 40–80% of 1961–90 mean flow, and winter increases of up to 20%. This changing seasonality has a large impact on low flows, with Q_{95} projected to decrease in magnitude by 40–80% in summer months, with serious consequences for water abstractions and river ecology. In contrast, high flows ($> Q_5$) are projected to increase in magnitude by up to 25%, particularly at high elevation catchments, providing an increased risk of flooding during winter months. These changes will have

implications for management of water resources and ecologically important areas under the EU Water Framework Directive.

Wang, Chen, Shi and Gelder2 (2008) has mentioned that the extreme hydro-meteorological events have become the focus of more and more studies in the last decade. Due to the complexity of the spatial pattern of changes in precipitation processes, it is still hard to establish a clear view of how precipitation has changed and how it will change in the future. In the present study, changes in extreme precipitation and streamflow processes in the Dongjiang River Basin in southern China are investigated with several nonparametric methods, including one method (Mann-Kendall test) for detecting trend, and three methods (Kolmogorov–Smirnov test, Levene's test and quantile test) for detecting changes in probability distribution. It was shown that little change is observed in annual extreme precipitation in terms of various indices, but some significant changes are found in the precipitation processes on a monthly basis, which indicates that when detecting climate changes, besides annual indices, seasonal variations in extreme events should be considered as well. Despite of little change in annual extreme precipitation series, significant changes are detected in several annual extreme flood flow and low-flow series, mainly at the stations along the main channel of Dongjiang River, which are affected significantly by the operation of several major reservoirs. To assess the reliability of the results, the power of three non-parametric methods are assessed by Monte Carlo simulation. The simulation results show that, while all three methods work well for detecting changes in two groups of data with large sample size (e.g., over 200 points in each group) and large differences in distribution parameters (e.g., over 100% increase of scale parameter in Gamma distribution), none of them are powerful enough for small data sets (e.g., less than 100 points) and small distribution parameter difference (e.g., 50% increase of scale parameter in Gamma distribution). The result of the present study raises the concern of the robustness of statistical change-detection meth-ods, shows the necessity of combined use of different methods including both exploratory and quantitative statistical methods, and emphasizes the need of physically sound explanation when applying statistical test methods for detecting changes.

Chapter-3

STUDY AREA

3.1 General

Koraput district is full of natural beauty, which fills one's heart with immense joy. The historical background of this district is very much influenced by its rare gifts of nature. A vast stretch of hilly region, charming valleys, perennial streams, waterfalls and deep forests have attracted some aboriginal races like the Marias, the Gadabas and the Bondas and given them shelter in its lap. Being virtually cut off from the main stream of cultural developments of other parts of the state, they till now mostly follow the primitive method of cultivation, pottery, basket-making, spinning and weaving. They also erect memorial stones in religious places and graveyards.

3.2 Agricultural

The Sabari sub-basin includes Koraput district, this is known as one of the centers of origin of rice. The people of Koraput district, notably the adivasis have generated and conserved many indigenous cultivars of rice that are suitable for both dry-land and wetland cultivation. The Food and Agricultural Organisation (FAO) in 2012 recognised the service of the communities of Koraput in ensuring food security by declaring the Koraput district as a Global Agricultural Heritage Site. In 2006 the Ministry of Panchayati Raj named Koraput one of the country's 250 most backward districts (out of a total of 640). It is one of the 19 districts in Odisha currently receiving funds from the Backward Regions Grant Fund Programme (BRGF).

3.3 Rainfall:

Monsoon sets in around middle of June (or sometimes late May) and continues till September (sometimes up to October]. Nearly 80% of the rainfall is received from the southwest Monsoon. During the monsoon the wind direction is from west or south west. Regions on the wind-ward side (western side of the hills) receive more rains than others. Thus the rainfall in Jeypore and Malkangiri zones is heavier than in Rayagada. The annual average rainfall in the district was 1521.8 mm between 1901 and 1950. The average in the decade between 1951 and 1960 was 1652.2 mm. The mean annual rainfall between 1975 and 1980 was 1430.6 mm. The average rainfall for the district in these seven years is 1353.5 mm and this indicates a declining trend from the middle of the present century. This is probably due to the gross ecological changes brought about by gradual deforestation for the purpose of slash and burn type of cultivation

(Chandrasekeren, 1983). The rainfall in Jeypore and Malkangiri zones were nearly the same, though year to year variations were observed. Rayagada zone being on the lee-ward side, receives minimum rainfall. The study are contains three rainfall station namely Jaypore, Koraput and Malagankiri and one gauge station at Saradaput. The study area is shown in Fig. 3.1.

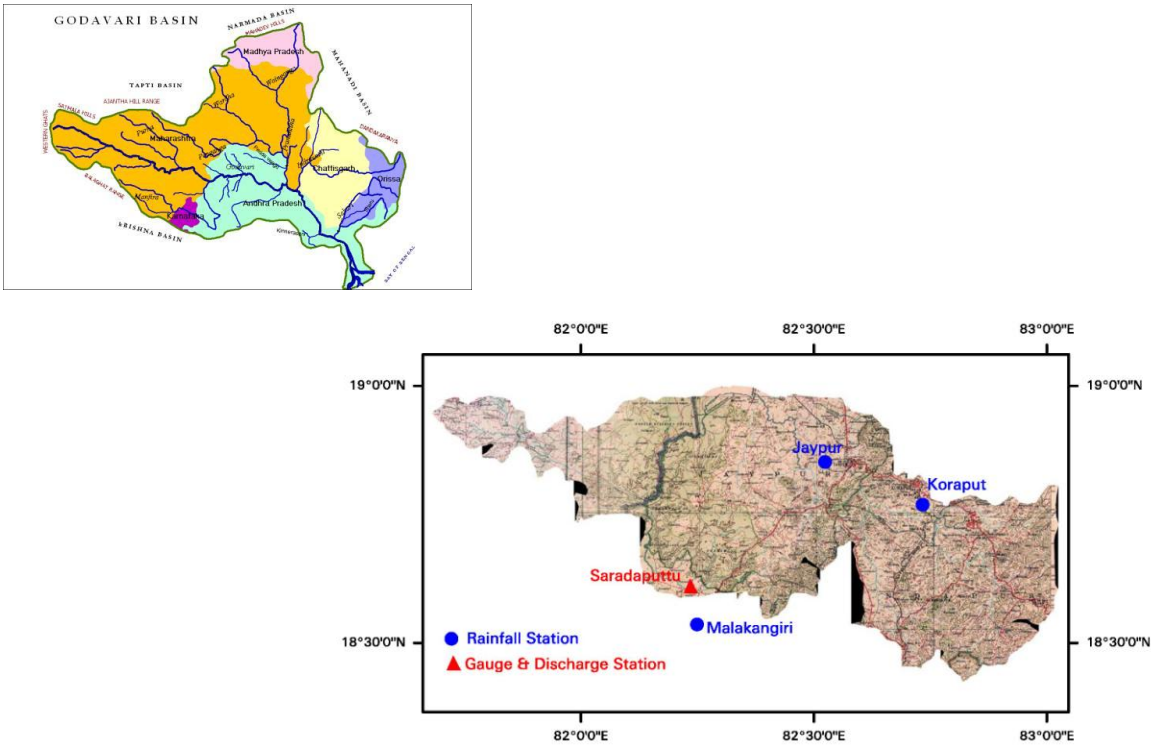

Fig. 3.1Study Area – Sabari Sub-basin (Catchment area – 4719.55 Sq.km)

3.4 Temperature:

The climate in the study area is generally hot between March to May and the highesttemperature was recorded in the month of May in all the parts of Sabari sub-bsin. In June, there was a decrease In temperature following the onset of rains. The temperature was considerably low during November to February, December being the coolest part of the year. While these seasonal changes were similar all over the study area, there were some variations in different

zones. Koraput zone had the coolest climate with minimum temperature recording 6.5^{o} C in December and maximum of 35.4^{o} C in May. While the climate of Jeypore zone was intermediate. Rayagada and Malkangiri zones are hotter. The mean maximum temperature recorded was upto 43.7 ^{o} C and 42.9 ^{o} C.

3.5 Physiography

The hills of the eastern ghats lie to the north west of Rajmndry and Vishakhapatnam and rise almost abruptly from sea level to heights of about 900 to 1200 meters. The famous Jeypore hills of Koraput district forms the northern most part of these hill ranges and is continuous with those in the adjoining districts of Andhra Pradesh (Vishakhapatnam, East Godavari and Madhya Pradesh (Bastar district). The study area is highly undulating one, covered with many hills, forests and is crisscrossed with numerous perennial and seasonal streams and channels. The physiography of the district not uniform and is divided into 4 zones on the basis of altitude, separated by natural barriers. They are Ester Koraput Zone, Jeypore Zone, Rayagada Zone and the Malkangiri Zone.

3.6 Soils

Four varieties of soil are found in thestudy area. They are as follows: i) Red laterite soil: this is the common type of soil found in the whole of Koraput district and particularly abundant in Koraput and Jeypore zones. ii) Black soil is found in Malkangiri zone and in some parts of Jeypore zone (Umerkote). This is black in colour, contains large quantities of organic matter and is more fertile compared to red laterite. iii) Alluvial soil is found on either side of Indravathi in Jeypore zone (Borigumna, Kotpad and Nawarangapur areas) and on either side of Vamsadhara in Rayagadd zone. This soil is rich in organic matter and is quite fertile. iv) Sandy soil is found in some parts of Rayagada zone and few pockets in Koraput zone.

3.7 Mineral resources and forest

The Sabari sub-basin is very rich in mineral deposits and forest wealth. It has large deposits of iron ore, high grade bauxite, lime stone of best cement grade quality and also sizable deposits of mica, tin and other metals. The study area is abundant in forest wealth, which forms an important source of livelihood for the tribals. A total of 12,219 sq.km. of area in the koraput district is under forest cover (approximately 50% of total area) and the forest contributes to about 61% of total revenue of the district. The major forest produce is timber, which includes Sal (E.Robusta) , Piasal, Saguan (Tectona grandis), Sahaj (Terminalis tomentosa) , Teak and Bamboo. The minor forest products include tamarind, hlahua flowers, Sal seeds and resins, barks, soap nut. arrow roots, wax, Kendu (Diospyros melanosylon) or Beedi leaves, broms, silk cotton, medicinal plants, canes, honey, gooseberry etc. These products are not only supplied to different parts of India, but also overseas (Chandrasekeren, 19831).

Chapter-4
METHODOLOGY

4.1 General

The ARNO model, given its simplicity and robustness, was used in various parts of the world as the basic tool for the development of several real-time operational flood forecasting systems. Moreover, the soil moisture balance component was successfully used as an alternative to the Manabe (1969) soil bucket in the several GCMs, such as the ECHAM2 model (Dümenil and Todini, 1992, Roeckner et al., 1992), the UK Meteorological Office (UKMO) model (Rowntree and Lean, 1994), and the LMD model (Polcher et al., 1995). ARNO model is also employed in land-surface-atmosphere process research and as a tool for investigating land use changes.

The ARNO rainfall-runoff model (Todini, 1996) was originally developed as part of a real time flood forecasting system for River Arno (Italy). Input data required by ARNO model are: topographic data (hill-slope and channel slopes), precipitation, temperature and river levels at several stations within the catchment, soil type and land use data and rating curves for hydrometric stations where the discharge is to be simulated. The methodology used in ARNO model is relatively straightforward process since the model parameters have clearly defined effects on catchment response. The ARNO model is a variable contributing area semi-distributed conceptual model with two main components: the first one describes the soil moisture balance, while the second one describes the transfer of runoff to the outlet of the basin.

4.2 Representation of hydrological processes

The main physical phenomena represented in the model are: the water balance in the soil, the water losses through evapo-transpiration, snow melt, overland flow, groundwater flow and channel flow routing. These processes have been developed into the model as inter-linked modules. The soil moisture balance is determined by dividing the catchment into elements classified as pervious or impervious, and then assuming that a distribution function can describe the proportion of pervious area that is saturated.

– precipitation. Rainfall and temperature inputs are provided to the model as area averages by means of weights generally based upon Thiessen polygons for rainfall, and taking into account of thermal gradient with elevation for temperature.

– snow melt and accumulation. The snowmelt module is driven by a radiation factor estimated from air temperature measurements. The sub-catchment area is subdivided into equi-elevation zones to take account of the role that altitude may play in combination with the thermal gradient. Snow accumulation and/or melt are based on the energy balance of the snow cover (when present) as a function of air temperature and precipitation.

– evaporation and transpiration. Evapo-transpiration is assumed to depend on: crop, wind speed, temperature, altitude, extraterrestrial radiation and the proportion of sunshine. The calculation of evapo-transpiration is based on a simplified form of the Penman-Monteith equation.

– infiltration. Infiltration is expressed by an empirical relationship as a non-linear function of the soil moisture content.

– base-flow. It is generated by the presence of a groundwater table fed by the percolation, and computed by the groundwater module.

– channel routing. The channel routing is also performed by means of a distributed input linear parabolic model, and the contribution from upstream sub-catchments is routed downstream by means of a linear concentrated-input parabolic model.

– surface runoff. Once the runoff is obtained from the soil moisture balance, the routing of runoff on the hill-slopes of the watershed is simulated by applying a distributed inflow linear parabolic model to an “open book” representation of the hill-slope elements.

4.3 Soil Moisture Balance Module

As pointed out by Dooge (1973) and also shown by Todini and Wallis (1977) the major problem in representing the rainfall runoff process lies in the strongly non-linear behaviour and feed-back due to the soil moisture storage, which controls the runoff production. This is why the different rainfall runoff are qualified and distinguished on the basis of the soil moisture balance

representation they adopted. The soil moisture balance module of the ARNO model derives from the Xinanjiang model developedby Zhao (1977, 1984), who expressed the spatial distribution of the soil moisture capacity in the form of a probability distribution function, similar to that advocated by Moore and Clarke (1981) and Moore (1985). Successively, in order to account more effectively for soil depletion due to drainage, this model scheme was modified by Todini (1988), who originated the ARNO model within the frame of the hydrological study of the river Arno. The basic assumptions expressed in the soil moisture balance module of the ARNO model are:

- the precipitation input to the soil is considered uniform over the catchment (or sub-catchment) area;
- the catchment is composed of an infinite number of elementary areas (each with a different soil moisture capacity and a different soil moisture content) for each of which the continuity of mass can be written and simulated over time;
- all the precipitation falling over the soil infiltrates unless the soil is either impervious or it has already reached saturation; the proportion of elementary areas which are saturated is described by a spatial distribution function;
- the spatial distribution function describes the dynamics of contributing areas which generate surface runoff;
- the total runoff is the spatial integral of the infinitesimal contributions deriving from the different elementary areas;
- the soil moisture storage is depleted by the evapo-transpiration, by lateral sub-surface flow (drainage) towards the drainage network and by the percolation to deeper layers;
- both drainage and percolation are expressed by simple empirical expressions.

A sub-basin of given surface area S_T (excluding the surface extent of water bodies such as reservoirs or lakes) is in general formed by a mixture of pervious and less pervious soils, the response to precipitation of which will be substantially different. For this reason the total area S_T is divided into the impervious area S_I and the pervious area S_P :

$$S_T = S_I + S_P \qquad (1)$$

In order to derive the expressions needed for the continuous updating of the soil moisture balance, let us first deal with the amount of precipitation that falls over the pervious area. Given that from equation (1) the entire pervious area is:

$$S_p = S_r + S_i \tag{2}$$

if one denotes by (S - SI) the generic surface area at saturation, x, defined as:

$$x = \frac{S + S_i}{S_r + S_i} \tag{3}$$

will indicate the proportion of pervious area at saturation. Zhao (1977) demonstrated that the following relation holds reasonably well between the area at saturation and the local proportion of maximum soil moisture content w/wm, where w is the elementary area soil moisture at saturation and wm is the maximum possible soil moisture in any elementary area of the catchment.

$$x = 1 - \left(1 - \frac{w}{w_m}\right)^b \tag{4}$$

This can be inverted to give the cumulative distribution for the elementary area soil moisture at saturation:

$$W = w_m \left[1 - (1 - x)^{\frac{1}{b}}\right] \tag{5}$$

In the ARNO model, an interception component (Rutter et.al., 1971, 1975) is not explicitly included. Nevertheless in order to allow for a substantially larger evapotranspiration when the canopies are wet (without obviously explicitly accounting for the disappearance of the stomatal resistance (Shuttleworth, 1979)), the following succession of operations is followed.

If the precipitation P is larger than the potential evapotranspiration ETp, the actual evapotranspiration, for the reasons expressed above, is assumed to coincide with the potential, i.e.:

$$ET_a = ET_p \tag{6}$$

and so an "effective" meteorological input Me , defined as the difference between precipitation and potential evapo-transpiration, becomes:

$$M_e = P - ET_a = P - ET_p > 0 \tag{7}$$

The surface runoff R generated by the entire catchment is obtained as the sum of two terms, the first one is the product of the meteorological effective input and the percentage of impervious area while the second one is the average runoff produced by the pervious area, which is obtained by integrating the soil moisture capacity curve, which gives:

If the precipitation P is smaller than the potential evapotranspiration ET_p the effective meteorological input M_e, becomes negative:

$$M_e = P - ET_p < 0 \qquad (8)$$

which implies that the runoff R is zero. The actual evapotranspiration is then computed as the precipitation P plus a quantity which depends upon Me reduced by the average degree of saturation of the soil, which gives:

$$E\ T_a = P + \left(E\,T_p - P\right)\left(\frac{S_T - S_1}{S_r}\right)\frac{\left(1+\frac{W}{Wm}-\frac{1}{b}\right)-\left(1-\frac{W}{W_m}\right)^{\frac{1}{b+1}}}{\left(1+\frac{1}{b}\right)-\left(1-\frac{W}{W_m}\right)^{\frac{1}{b+1}}} \qquad (9)$$

These equations, which represent the average surface runoff produced in the sub-catchment, must be associated with an equation of state in order to update the mean water content in the soil. This equation takes the form:

$$W_{t+\Delta t} = W_t - P - ET_a - R - D - I \qquad (10)$$

where all the quantities represent averages over the sub-basin and are expressed in mm:

Wt+Δt is the soil moisture content at time t+Δt;

Wt is the soil moisture content at time t .

P is the area precipitation between t and t+Δt;

ETa is the evapotranspiration loss between t and t+Δt;

R is the total runoff between t and t+Δt;

D is the loss through drainage between t and t+Δt;

I is the percolation loss between t and t+Δt;

The non-linear response of the unsaturated soil to precipitation, represented by the shape of the distribution curve given by equation (5), is strongly affected by the horizontal drainage and

vertical percolation losses. The drainage loss D is an important quantity to be reproduced in a hydrological model, since on the one hand it affects the soil moisture storage and on the other hand it controls the hydrograph recession. Theoretical considerations on the unsaturated zone flow as well as application results have suggested in time various types of empirical relationships to express the drainage loss D as a non- linear function of the soil moisture. The most recently adopted expression in the ARNO model is the following, which although written as a lumped equation valid at catchment scale, looks similar to the one, valid at a point, which is due to Brooks and Corey (1964):

$$D = D_s\left(1 - \frac{w}{w_m}\right)^b \qquad (11)$$

Where

W

W_m is the percentage saturation;

c1 is an exponent related to the soil types;

D_s is the drainage at saturation;

The percolation loss *I*, which feeds the groundwater module, is represented with a similar expression, although generally with different parameters. which will control the base flow in the model, varies less significantly over time if compared with the

other terms; nevertheless a non-linear behavior.

The total runoff per unit area produced by the precipitation P is finally expressed as:

$$R_{tot} = R + D + B \qquad (12)$$

where:

B is the base flow generated by the presence of a groundwater table fed by the percolation, and computed by the groundwater module.

4.4 The Evapotranspiration Module:

In the ARNO model, a second forcing factor is provided by evapotranspiration, which can be either computed externally and directly introduced as an input to the model or estimated internally as a function of the air temperature. The internal evapotranspiration estimator uses in fact a simplified technique which has proven more than accurate for modelling the rainfall runoff

process, where evapotranspiration plays a major role not really in terms of its instantaneous impact, but in terms of its cumulative temporal effect on the soil moisture volume depletion; this reduces the need for an extremely accurate expression, provided that its integral effect be well preserved. Although acknowledging the fact that the Penman-Monteith equation is the most rigorous theoretical description for this component, for a practical utilisation a simplified approach is generally necessary because in most countries the required historical data for its estimation are not extensively available, and, in addition, apart from a few meteorological stations, almost nowhere are real time data available for flood forecasting
applications. In the ARNO model, the effects of the vapour pressure and wind speed are explicitly ignored and evapotranspiration is calculated starting from of a simplified equation known as the radiation method (Doorembos et al., 1984):

$$E\ T_{0d} = C_v W_{ta} R_s = C_v W_{ta} \left(0.25 + .50 \frac{n}{N}\right) R_a \qquad (13)$$

where:

ET_{0d} is the reference evapotranspiration, i.e. evapo-transpiration in soil saturation conditions caused by a reference crop (mm/day) ;

C_v is an adjustment factor obtainable from tables as a function of the mean wind speed;

W_{ta} is a compensation factor that depends on the temperature and altitude;

R_s is the short wave radiation measured or expressed as a function of Ra in equivalent evaporation (mm/day);

R_a is the extraterrestrial radiation expressed in equivalent evaporation (mm/day);

n/N is the ratio of actual hours of sunshine to maximum hours of sunshine (values measured or estimated from mean monthly values).

Hence the calculation of R_s requires both knowledge of R_a, obtainable from tables as a function of latitude, and knowledge of actual n/N values, which may not be available. In the absence of the measured short wave radiation values R_s or of the actual number of sunshine hours otherwise needed to calculate R_s as a function of R_a (see equation (18)), an empirical equation was developed that relates the reference potential evapotranspiration ET_{0d}, computed on a monthly basis using one of the available simplified expressions such as for instance the one due to Thornthwaite and Mather (1955), to the compensation factor W_{ta}, the mean recorded temperature

of the month T and the maximum number of hours of sunshine N. The developed relationship is linear in temperature (and hence additive), and permits the disaggregation of the monthly results on a daily or even on an hourly basis, while most other empirical equations are ill-suited for time intervals shorter than one month. The relation used, which is structurally similar to the radiation method formula in which the air temperature is taken as an index of radiation, is:

$$ET_0 = \alpha + \beta\ NWtaTm \qquad (14)$$

where:

ET_0 is the reference evapotranspiration for a specified time step Δt (in mm/Δt);

α,β are regression coefficients to be estimated for each sub-basin;

Tm is the area mean air temperature averaged over Δt;

N is the monthly mean of the maximum number of daily hours of sunshine (tabulated as a function of latitude). Wta for a given sub-basin can be either obtained from tables or approximated by a fitted parabola:where:

A, B, C are coefficients to be estimated;

T is the long term mean monthly sub-basin temperature (oC).

4.5 THE ARNO MODEL PARAMETERS

All the ESMA type models require calibration of several of parameters. Some of these parameters relate to the main processes, such as the soil moisture dynamical balance, and play an important role in the model performances in that they may modify the output by an order of magnitude. Other parameters, such as for instance the routing parameters, will only affect the timing of the response or may produce errors of the order of 10- 20%. This is why the comparison among the different ESMA type models, is generally based upon the soil component parameters.

In the ARNO model, the following parameters are soil component parameters that require accurate calibration by means of historical data and verification using split sample testing techniques:

W_m - represents the average volume in mm of soil moisture storage. This parameter can be derived as a function of the soil types and its value ranges in general from 50 to 350 mm;

b - represents a shape factor for the soil moisture vs saturated areas curve; its value, which ranges between .01 and .5, is somehow related to the soil types and their spatial variability, but must be estimated from the data.

Ds is the maximum drainage (in mm per time unit) that should be expected when the soil is completely saturated; it is a function of many factors including the geo-morphological structure of the catchment, the soil types, the space and time scales of the problem, and must be estimated from the data.

c1 exponent (which depends on soil types with values ranging generally between 1.5 and 3) used to represent drainage when saturation is not reached which value is estimated

from historical data.

Is is the maximum percolation (in mm per time unit) that should be expected when the soil is completely saturated; similarly to Ds it depends upon several items and must be estimated from the data.

c2 exponent (which depends on soil types with values ranging generally between 1 and 2) used to represent percolation when saturation is not reached which value is estimated from historical data.

Other parameters appearing in the equations, such as ST, SP and SI, do not require estimation from historical data, but can be directly evaluated on the basis of geo-morphological, soil and land use maps.

The ARNO model is therefore essentially based upon 6 parameters, a small number when compared to more classical ESMA type models (generally more than 20 parameters), but still the double of the parameters required in the TOPMODEL (Beven and Kirkby, 1979). Moreover, although related to the problem physics, not all the ARNO model parameters can be directly estimated or derived from maps, which is the major model limitation when wishing to use the model on ungauged catchments.

As mentioned earlier, the estimation of the parameters relevant to the routing model components (hillslopes and channels) are not critical. A convectivity C and diffusivity D coefficient must be provided for each response function which value may be related to the dimensions, slopes and lengths of the individual sub-basins. In general very small values for D are assumed for the hillslopes, given the marked kinematic nature of the phenomenon; generally, D increases with the size of the river and with the inverse of the bottom slope. Table 1 gives an indication of the orders of magnitude of C and D.

Table 1 -Approximate initial guess for parameters C and D.

Landcover Type	C (m/s)	D (m^2/s)
Hill slopes	1-2	1-100
Brooks	1-3	100-1000
Rivers	1 - 3	1000-10000
Large rivers	1 - 3	10000-100000

Chapter-5

RESULTS & DISCUSSION

5.1 Trend analysis of climatic variables (Rainfall and Temperature) of Sabari sub-basin using Mann-Kendall Test for the historical data 1901-2009 (109 years).

On running the Mann-Kendall test for temperature data, the following results in Table 1 were obtained respectively for the 12 months. If the p value is less than the significance level α (alpha) = 0.05, H_0 is rejected. Rejecting H_0 indicates that there is a trend in the time series, while accepting H_0 indicates no trend was detected. On rejecting the null hypothesis, the result is said to be statistically significant. Table 1 indicates that the Null Hypothesis was not accepted for any month. This shows that statistically significant increasing trends were observed in the case of temperature at Sabari-sub basin. The null hypothesis is tested at 95% confidence level for both, precipitation and temperature data. In addition, to compare the results obtained from the Mann-Kendall test, linear trend analysis of temperature data were plotted for all the twelve months in Fig 5.1 (a) & (b). The computed mean monthly temperature during the summer season i.e March, April, May and June are 32.9, 34.9, 36.1, 33.1^{o}C respectively. The linear trend analysis of 109 years temperature data indicates increasing trend during month of May and July.

Table 1. Results of Mann-Kendall Test for the Temperature data of the Sabari sub-basin.

Month	Min. Value T^{o}C	Max. Value T^{o}C	Mann-Kendall Statistic (Z)	Sen's Slope	*p*-value	Trend (At 95% level of significance)
January	24.92	29.11	1.90	0.006	0.012	**Increasing Trend**
February	27.77	31.06	4.83	0.011	0.015	**Increasing Trend**
March	31.20	34.8	5.43	0.013	0.017	**Increasing Trend**
April	32.75	37.04	4.01	0.009	0.014	**Increasing Trend**
May	33.49	38.43	4.31	0.012	0.017	**Increasing Trend**
June	30.47	35.78	2.56	0.010	0.018	**Increasing Trend**
July	28.31	30.6	4.48	0.008	0.011	**Increasing Trend**
August	27.53	30.12	3.85	0.005	0.008	**Increasing Trend**
September	28.42	30.91	6.19	0.008	0.011	**Increasing Trend**
October	28.23	30.68	5.39	0.009	0.012	**Increasing Trend**
November	25.46	29.95	3.34	0.010	0.016	**Increasing Trend**
December	24.39	28.72	4.11	0.012	0.017	**Increasing Trend**

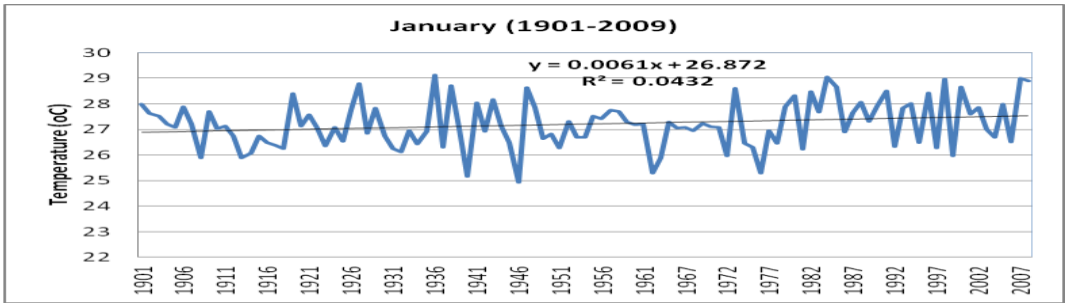

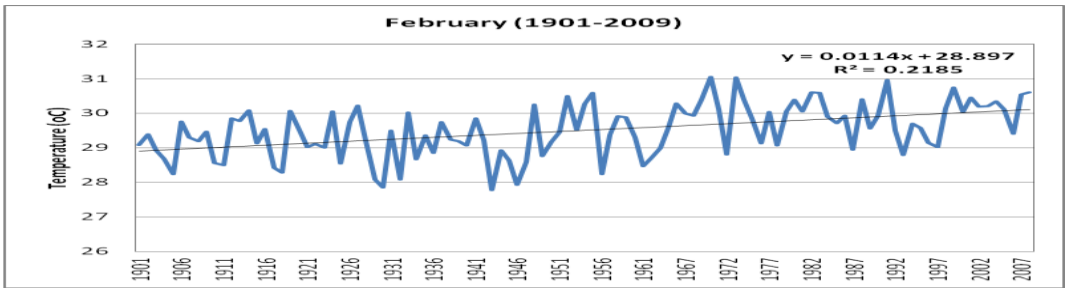

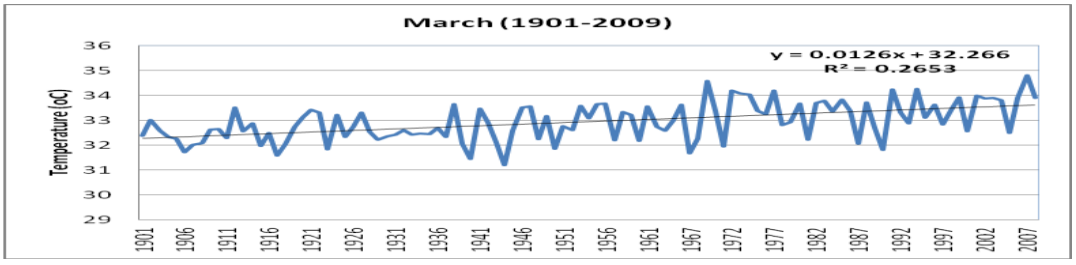

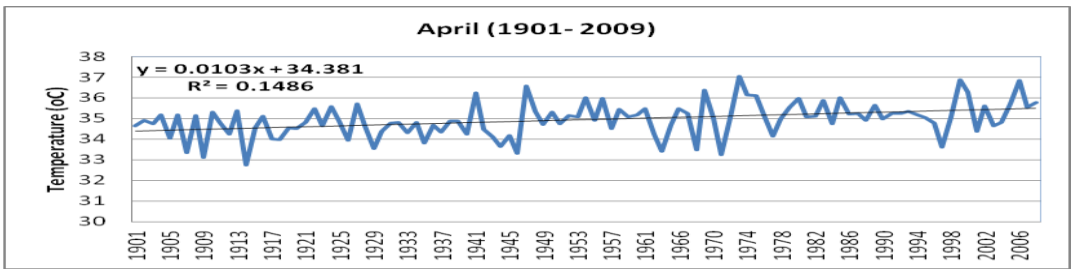

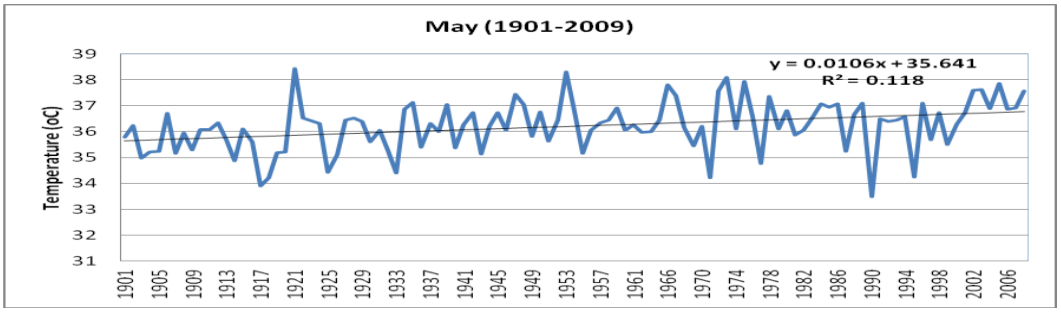

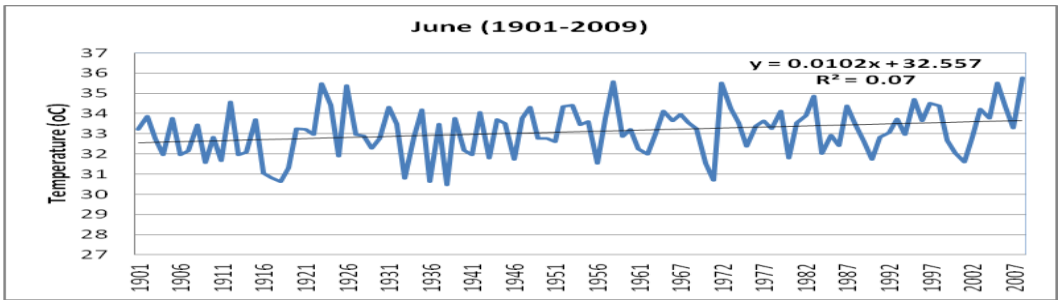

Fig. 5.1 (a) Linear Trend plots of Temperature data for the months January to June (1901-2009)

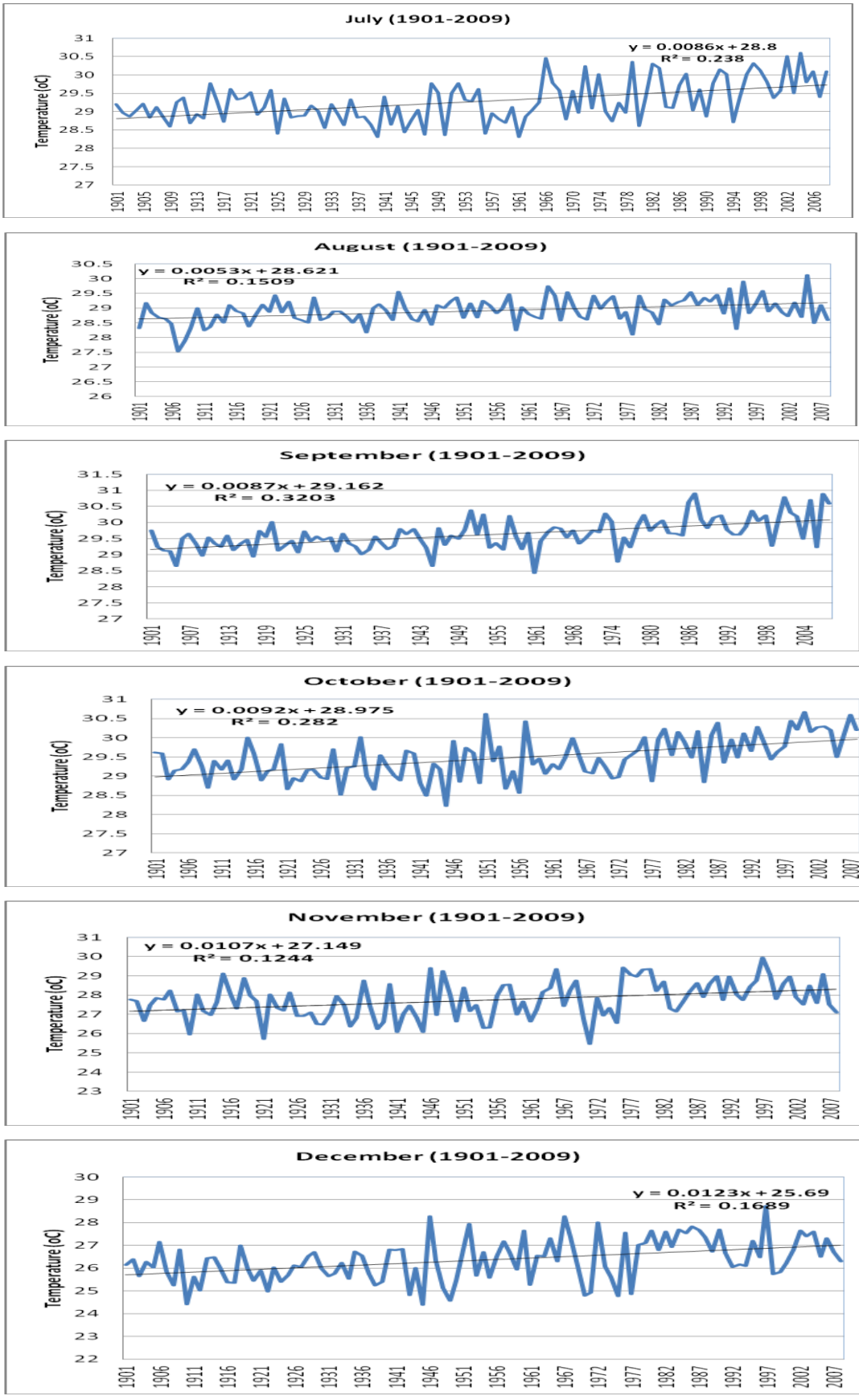

Fig. 5.1 (b)Linear Trend plots of Temperature data for the months July to December (1901-2009)

The Mann-Kendall test for precipitation data was carried out and the results are given below in Table 2. The results show that the trend indicator values are zero for the January and December months, therefore these two months exhibit no trend. The Sen's slope values are negative during February, March and September months. Therefore, these three months exhibit a decreasing trend in the rainfall pattern at the study area. The important monsoon months (June, July and August) have a positive trend indicator, however the significance level at 95% confidence is more than 0.05. Hence these three months show no trend phenomena. In addition, to compare the results obtained from the Mann-Kendall test, linear trend analysis of rainfall data were plotted for all the twelve months through Fig 5.2 (a) & (b). The computed average rainfall for the monsoon period i.e June, July, August and September are 174.48, 282.49, 291.61, 221.33mm respectively. Linear trend analysis of precipitation data shows that increasing trend during the month of June and decreasing trend during the month of September.

Table 2. Results of Mann-Kendall Test for the Precipitation data of the Sabari sub-basin.

Month	**Min. Value T^{o}C**	**Max. Value T^{o}C**	**Mann-Kendall Statistic (Z)**	**Sen's Slope**	***p*-value**	**Trend (At 95% level of significance)**
January	24.92	29.11	0.25	0.000	0.009	**No Trend**
February	27.77	31.06	-2.15	-0.004	0.000	**Decreasing Trend**
March	31.20	34.8	1.09	0.017	0.067	**No Trend**
April	32.75	37.04	-0.22	-0.016	0.153	**Decreasing Trend**
May	33.49	38.43	1.46	0.130	0.327	**No Trend**
June	30.47	35.78	1.51	0.396	0.890	**No Trend**
July	28.31	30.6	1.19	0.397	1.025	**No Trend**
August	27.53	30.12	0.89	0.279	0.878	**No Trend**
September	28.42	30.91	-1.39	-0.328	0.159	**Decreasing Trend**
October	28.23	30.68	1.17	0.267	0.709	**No Trend**
November	25.46	29.95	0.43	0.008	0.171	**No Trend**
December	24.39	28.72	0.25	0.000	0.009	**No Trend**

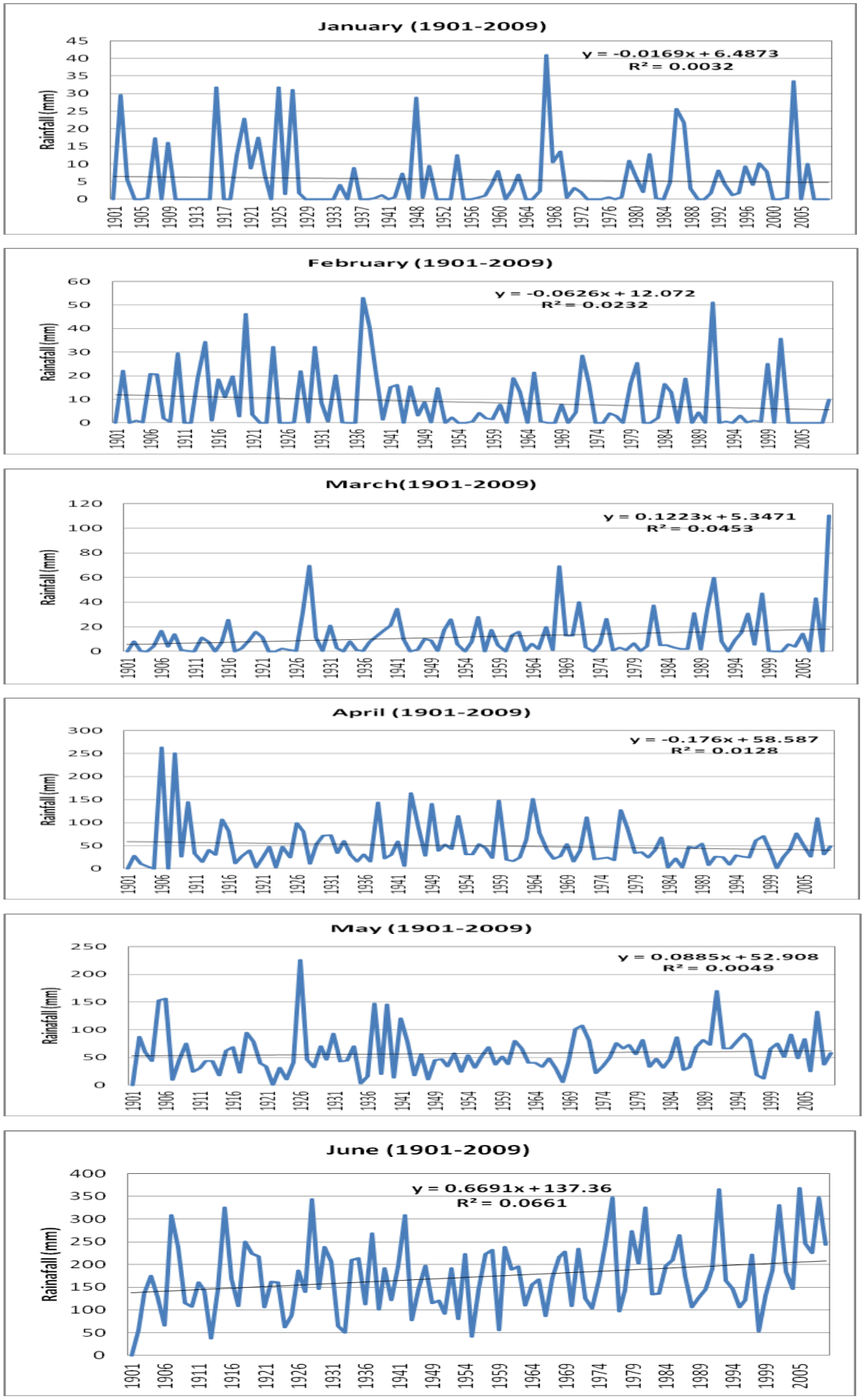

Fig. 5.2 (a) Linear Trend plots of Rainfall data for the months January to June (1901-2009)

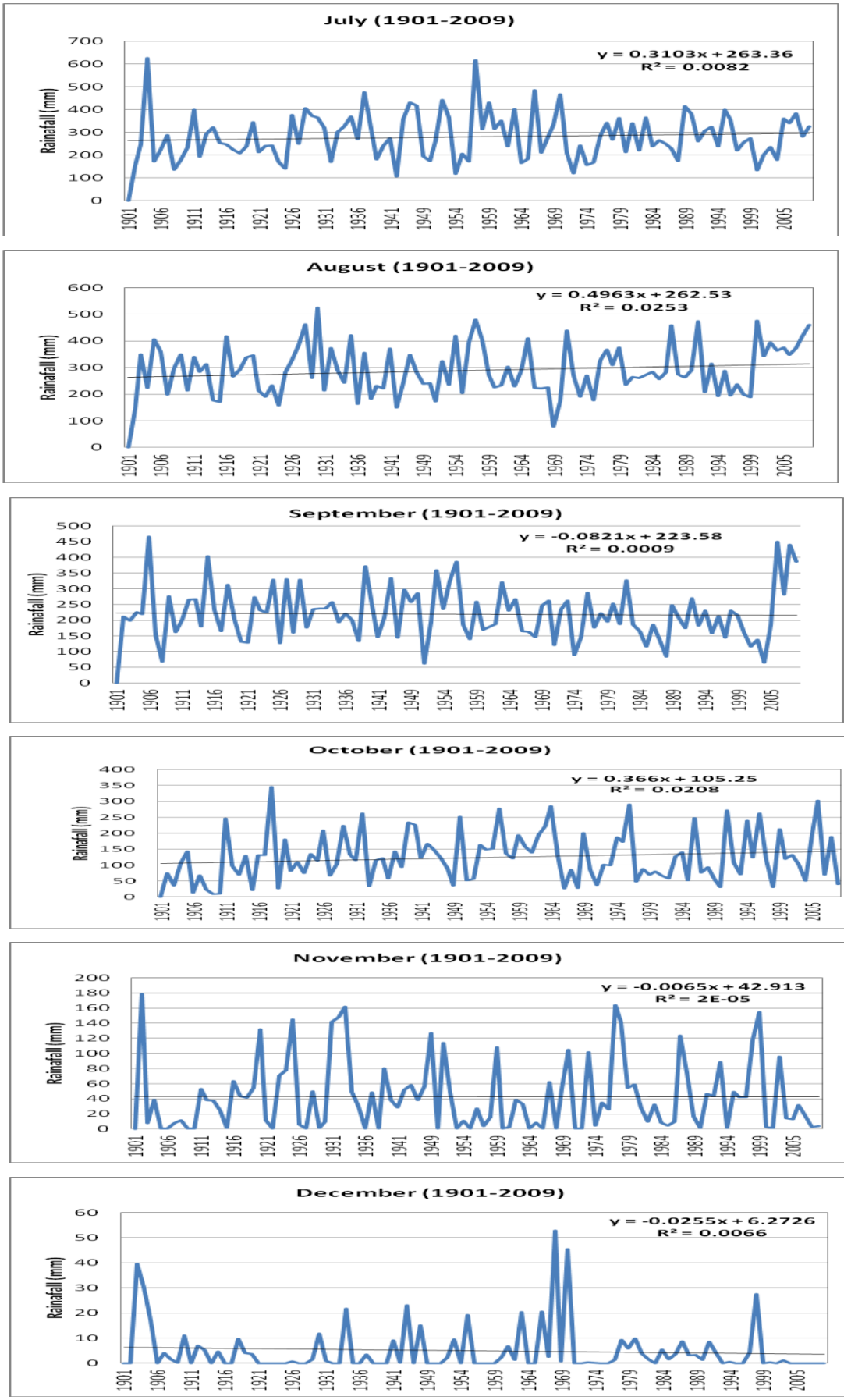

Fig. 5.2 (b) Linear Trend plots of Rainfall data for the months July to December (1901-2009)

5.2 **Rainfall-Runoff modeling of Sabari Sub-basin Using ARNO model:**

From the application point of view, several rivers have been successfully modeled by means of the ARNO model: the Fuchun river in China, the Danube river in Germany, and the rivers Arno, Tiber, Fortore, Ofanto, Adda, Ticino, Oglio, Agno- Guà, Tronto in Italy. In this study to assess the impact of climate change in Sabari sub-basin ARNO model was implemented using daily meteorological data for the period from 1970 to 2008 (38 years). The input data used in the ARNO model is rainfall, evapo-transpiration (ET) and discharge. Daily meteorological data were used for the model run. The evapo-transpiration was estimated using Hargreaves Method. The inputs required to estimate ET are potential extra-terrestrial radiation, minimum temperature and maximum temperature. The Hargreaves Method initially estimates reference crop-ET, downward solar (short wave) radiation (R_s), atmospheric emissivity, long wave radiation (R_L), and net radiation (R_{net}) before calculating the potential evapo-transpiration (PET) . The Sabari sub-basin comprises a geographical area of about 4719.55 sq.km. The sub-basin comprises three rainfall stations namely Jaypore, Malagangiri and Koraput. The gauge station is located at Saradaput. The ARNO model is based upon 6 parameters, a small number when compared to more classical ESMA type models (generally more than 20 parameters). The model parameters soil moisture storage ($W_{m),}$ shape factor for the soil moisture vs saturated areas curve (b), expected maximum drainage when the soil is completely saturated (D_s), c1 exponent (which depends on soil types with values ranging generally between 1.5 and 3), maximum percolation (I_s) and c2 exponent (which depends on soil types with values ranging generally between 1 and 2) were carefully used in the model run. The model was run for both the calibration (1970-1994) and validation (1995-2008). While running the calibration the above said parameters had been interchanged several times to get a reasonable output. After the calibration run the model parameters have been preserved and the same parameter values have been used for the validation run. The plots of calibration and validation run are shown in the Fig. 5.3. (a) and (b). The model efficiency during the calibration and validation run was 72.35% and 70.16% respectively.

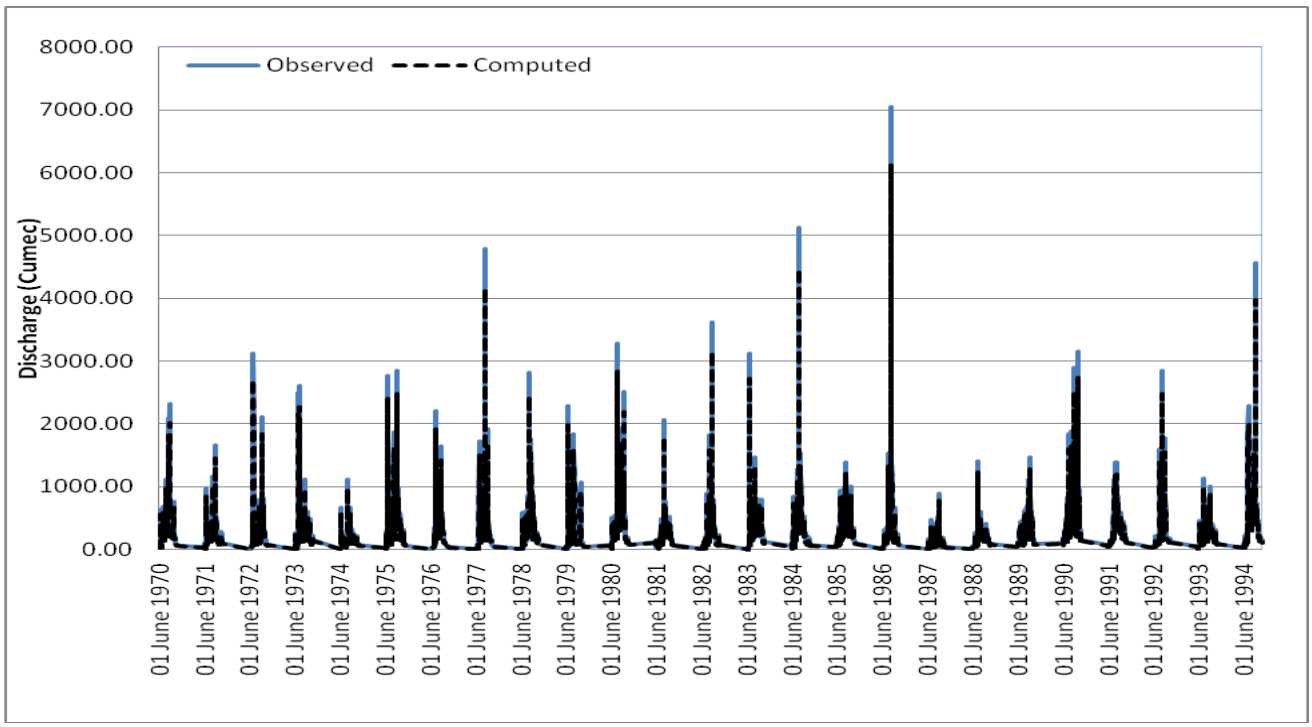

Fig.5.3 (a) Observed and Computed Discharge of Sabari sub-basin at Saradaput (Calibration 1970-1994)

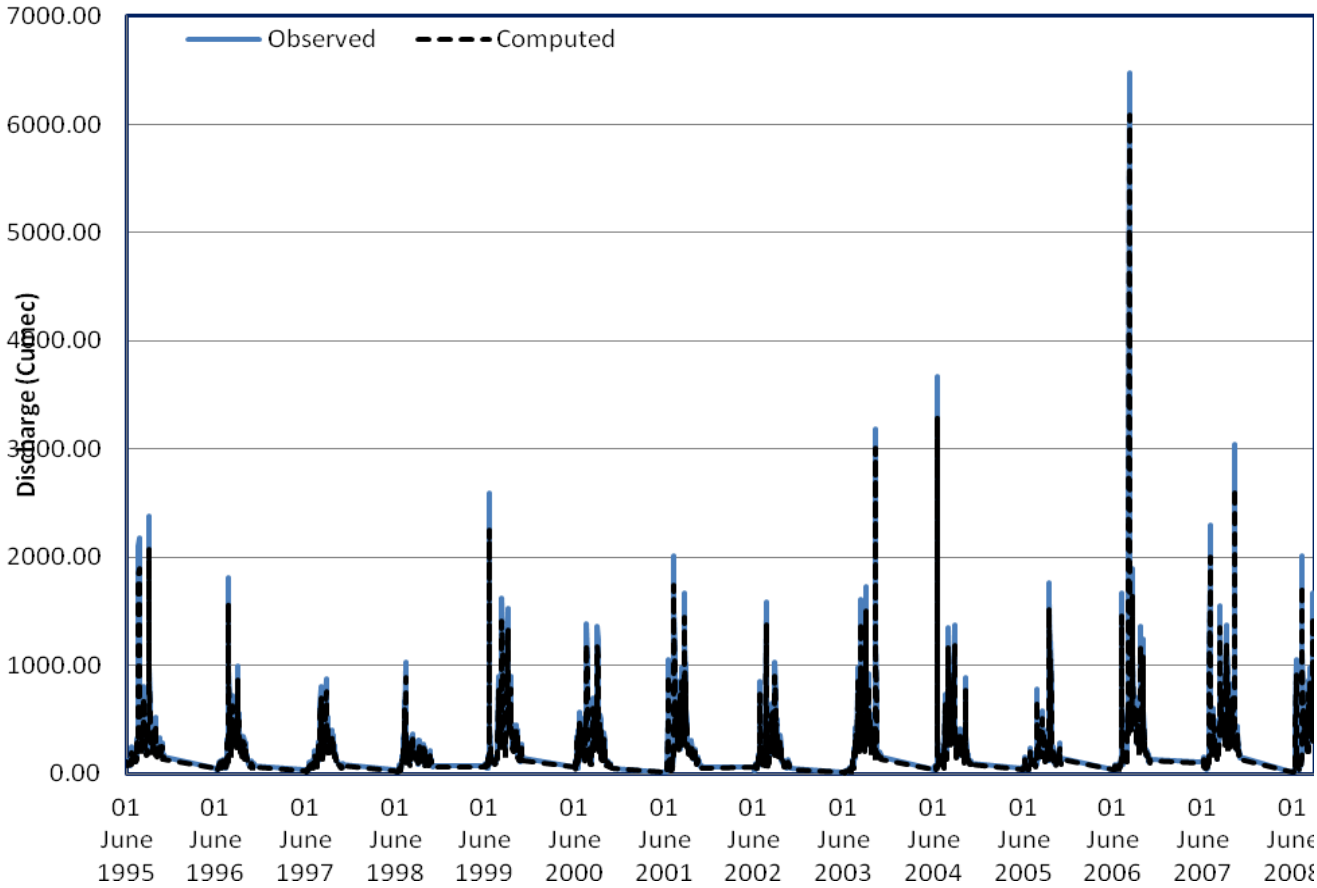

Fig.5.3 (b) Observed and Computed Discharge of Sabari sub-basin at Saradaput (Validation 1995-2008)

5.3 **Analysis of RCM downscaled data:**

Proving REgional Climate for Impact Studies (PRECIS) is an atmospheric and land surface model developed by UK's Met Office Hadley Centre portable regional climate model. PRECIS captures important regional information on summer temperature and monsoon rainfall data, which is missing in its parent Global Circulation Models (GCM). The Indian RCM PRECIS has been supplied by IITM, Pune. To study the impact of climate change on Sabari Sub-basin, the future climatic scenarios are required. It is a general practice to use a GCM and determine the futuristic scenarios. The grid size of a GCM model varies from 100 to 250 km. Therefore, GCM is not suitable for the sub-basin scale analysis. Hence, the RCM (Regional Climate Model) data which have a grid cell size of 50 km X 50 km has been used in this study. The RCM data received contains three different scenario periods i.) Base line period (1961 to 1990) ii.) Mid Century Period (2021 to 2050) and iii) End century period (2071 to 2098). All the three periods contains temperature and rainfall on daily basis.

5.3.1 Analysis of RCM downscaled temperature data (Daily Max.Temp) for the Baseline (1961-1990), Mid Century (2021-2050) and End Century (2071-2098) periods.

Temperature data received for the period 1961 to 1990 from RCM downscaled and IMD (Indian Meteorological Department) has been compared, which shows the maximum temperature observed by IMD during the summer season ranges from 35.4^{o} C to 38.3^{o} C. Whereas predicted temperature by RCM ranges from 46.94^{o} C to 48.6^{o} C. This shows that there is a huge variation between the observed and predicted values during the baseline period. The comparison between IMD and RCM downscaled data for the baseline period is shown in Fig. 5.4

Analysis of Mid Century (2021 to 2050) data revels that the maximum temperature during the summer season is alarmingly increases. The RCM data shows that the maximum temperature varies from 43.58^{o} C to 50.96^{o} C. From 2021 to 2032 the temperature varies from 43.58^{o} C to 49.52^{o} C, whereas from 2033 it increases from 50.10^{o} C and during the end of 2050 it touches 50.96^{o} C. The predicted maximum temperature values by RCM for the Mid Century period is shown in Fig. 5.5.

The same increasing trend continues for the End Century (2071 to 2098) period also. During this period the predicted data shows that the temperature various from 45.61^{o} C to 53.39^{o} C. The average maximum temperature during the End Century period is around 51^{o} C. From 2092 onwards the maximum temperature is above 53^{o} C. The predicted maximum temperature values by RCM for the End Century period is shown in Fig. 5.6.

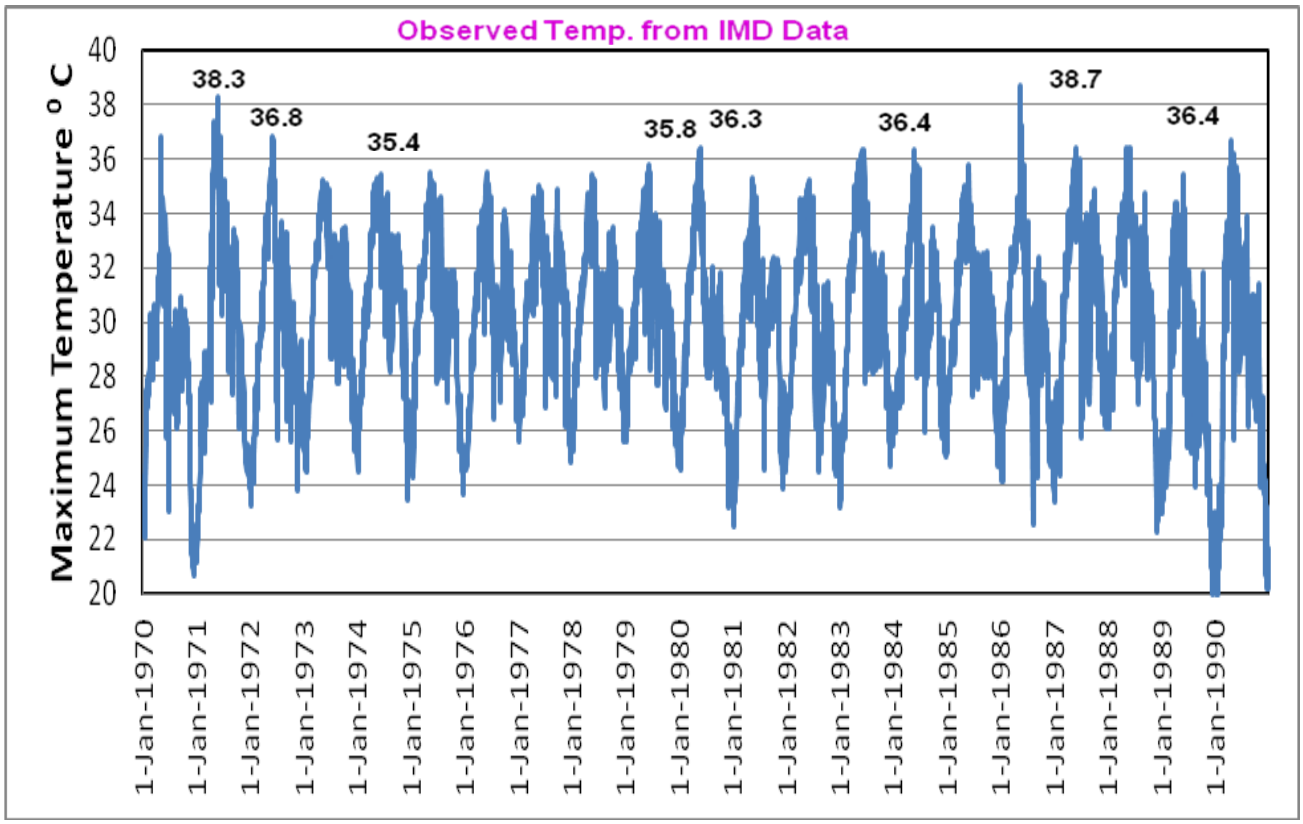

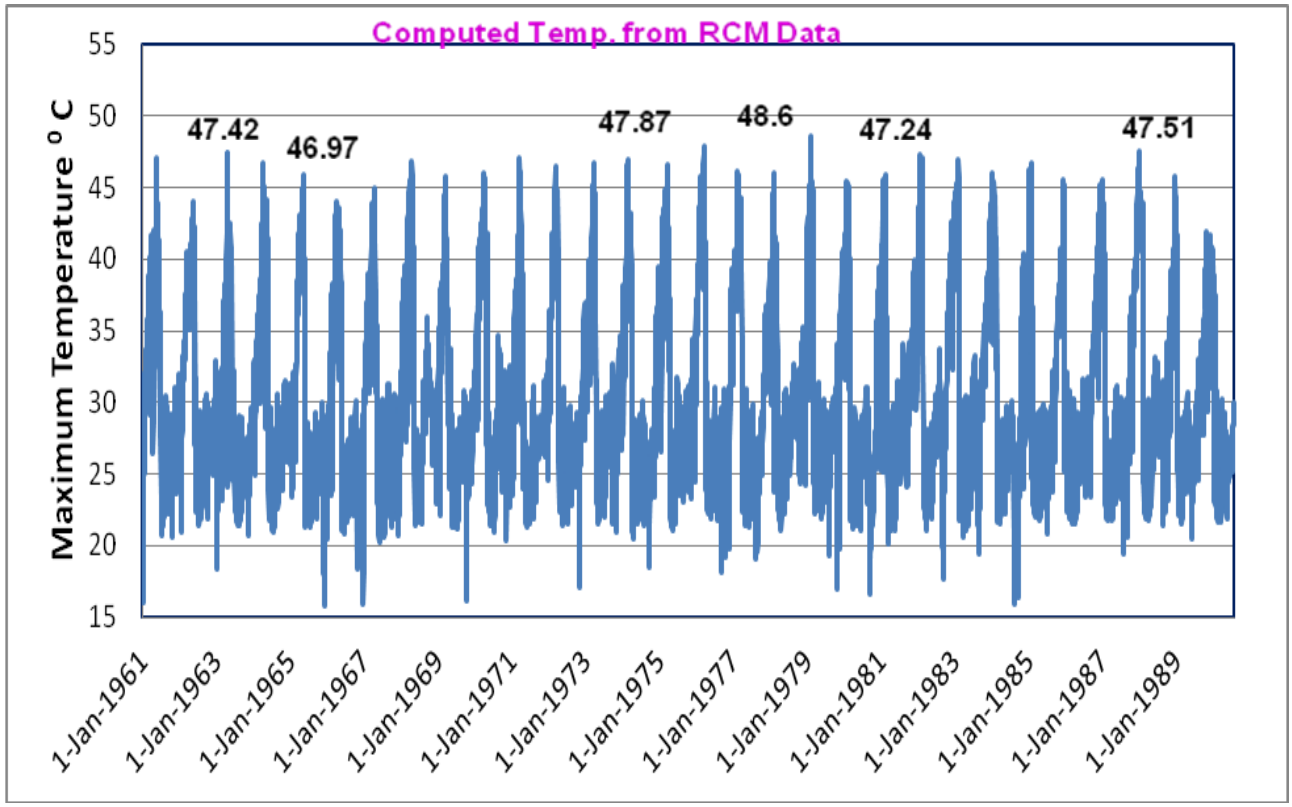

Fig.5.4 Comparison of IMD and RCM downscaled data (Daily Max.Temp) for the period 1961 to 1990

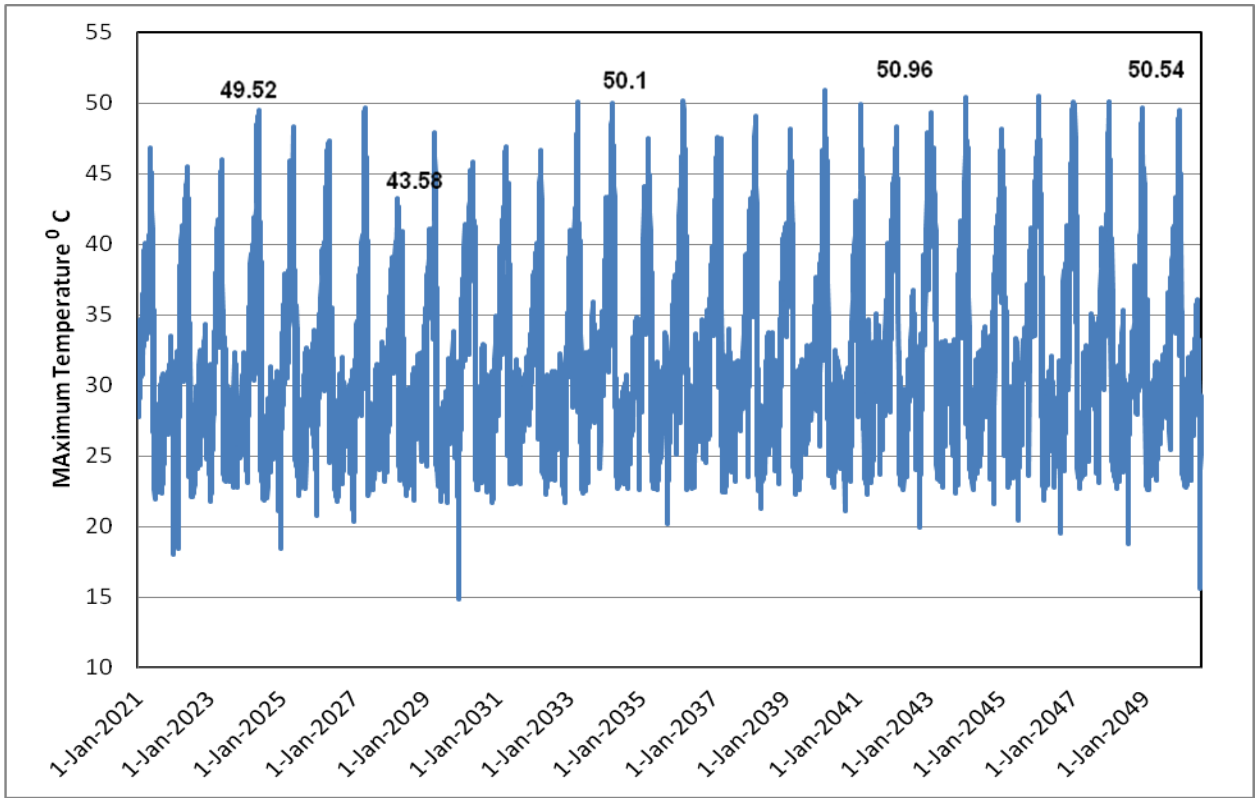

Fig.5.5 RCM downscaled data (Daily Max.Temp) for the period 2021 to 2050

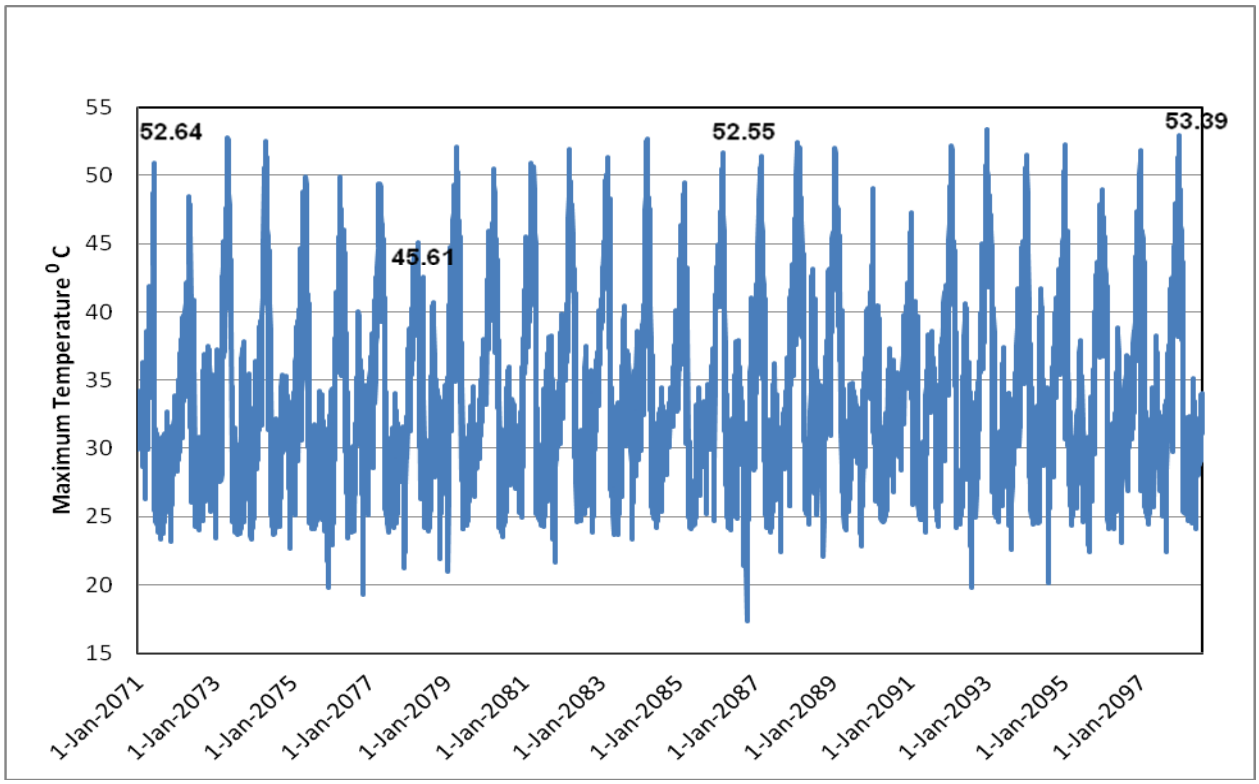

Fig.5.6 RCM downscaled data (Daily Max.Temp) for the period 2071 to 2098

5.3.2 Analysis of RCM downscaled daily Rainfall data for the Baseline (1961-1990), Mid Century (2021-2050) and End Century (2071-2098) periods.

Rainfall data received for the period 1961 to 1990 from IMD and RCM downscaled has been compared, which shows that the monthly rainfall observed by IMD ranges from 210.5 mm to 492.6 mm. Whereas predicted rainfall by RCM ranges from 400.2 mm to 1259.7 mm. This indicates that there is a huge variation between the observed and predicted values during the baseline period. The average monthly rainfall observed by IMD is around 300 mm, whereas the predicted value by RCM is around 800 mm. Analysis of IMD data reveals that the number of long spell rainfall events shows decreasing trend in monsoon season during the period 1961 to 1990. Whereas the short spell rainfall events with high intensity over the period show increasing trend. This creates frequent flood like situations in the study area. The comparison of monthly rainfall data between IMD and RCM downscaled data for the baseline period is shown in Fig. 5.7

Analysis of Mid Century (2021 to 2050) data revels that the rainfall events are alarmingly increasing with very high intensity in a short duration. This may cause frequent floods in the region and it may cause detrimental effects on landuse/landcover of the study area. Analysis of RCM downscaled data for the Mid Century reveals that the average monthly rainfall is around 800 mm. The minimum and maximum monthly rainfall is 286.2 mm and 1158.6 mm. The maximum rainfall during the mid century period is six times more than the maximum of the baseline period. The monthly RCM downscaled data for the Mid Century period is shown in Fig.5.8.

The same increasing trend continues for the End Century (2071 to 2098) period also with more peaks. The average monthly rainfall during the this period is around 850 mm. The minimum and maximum monthly rainfall is 465.6 mm and 1211.9 mm respectively. The monthly rainfall more than 1000 mm is increasing in this period. The monthly RCM downscaled data for the End Century period is shown in Fig.5.9.

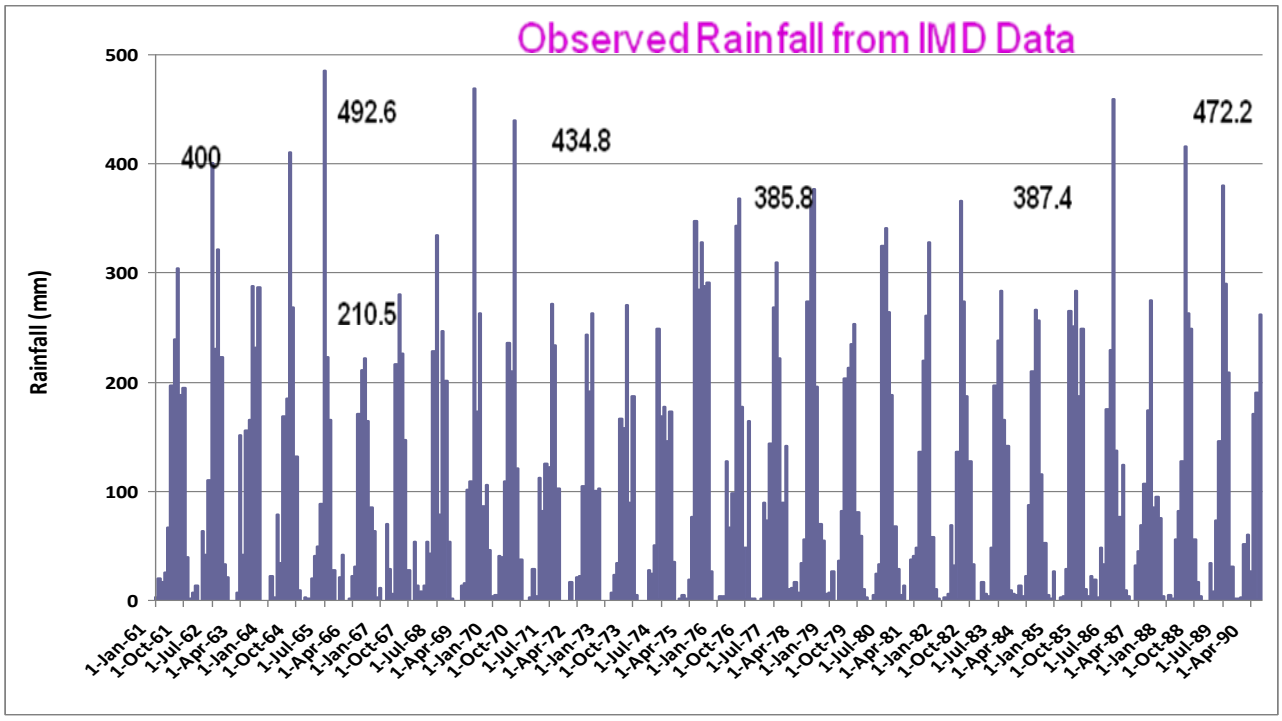

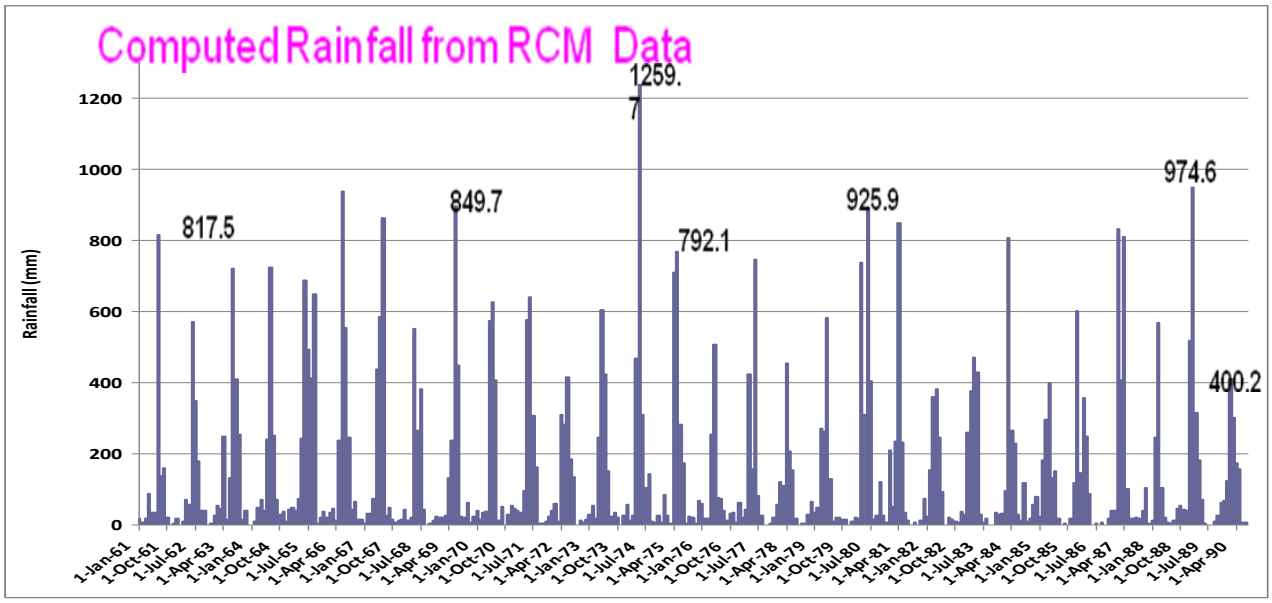

Fig. 5.7 Comparison of IMD and RCM downscaled data (Monthly Rainfall in mm) for the period 1961 to 1990

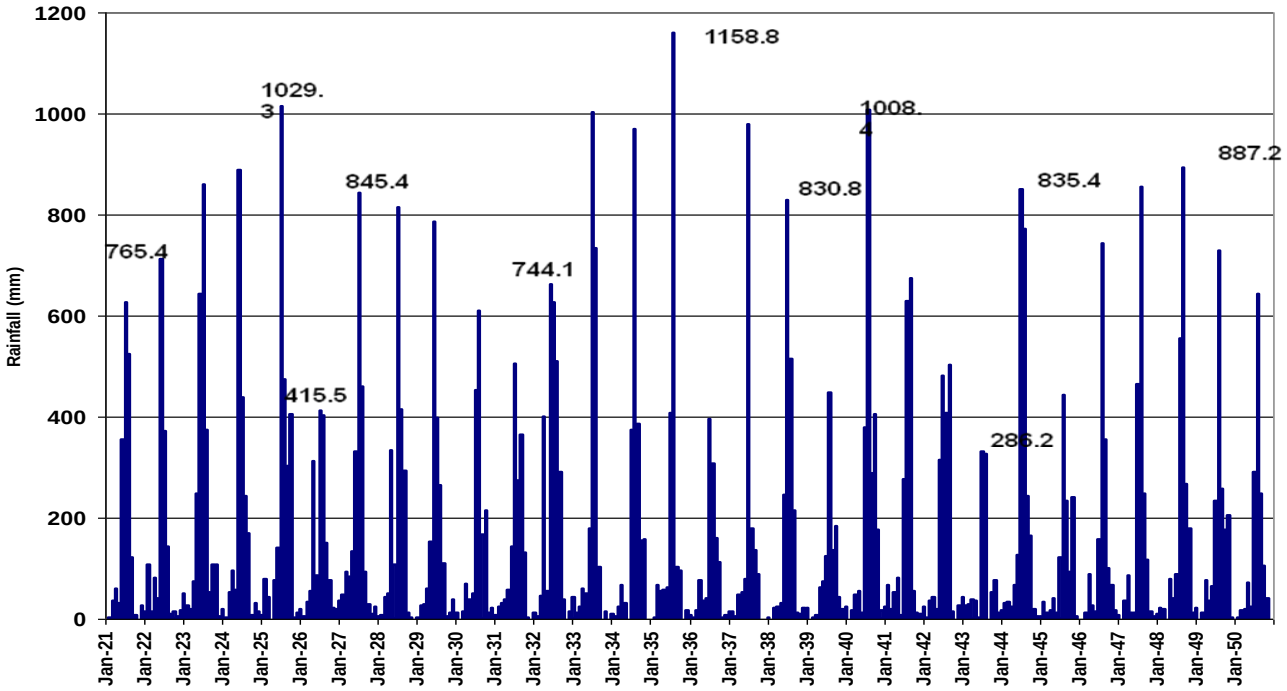

Fig.5.8 RCM downscaled data (Monthly Rainfall in mm) for the period 2021 to 2050

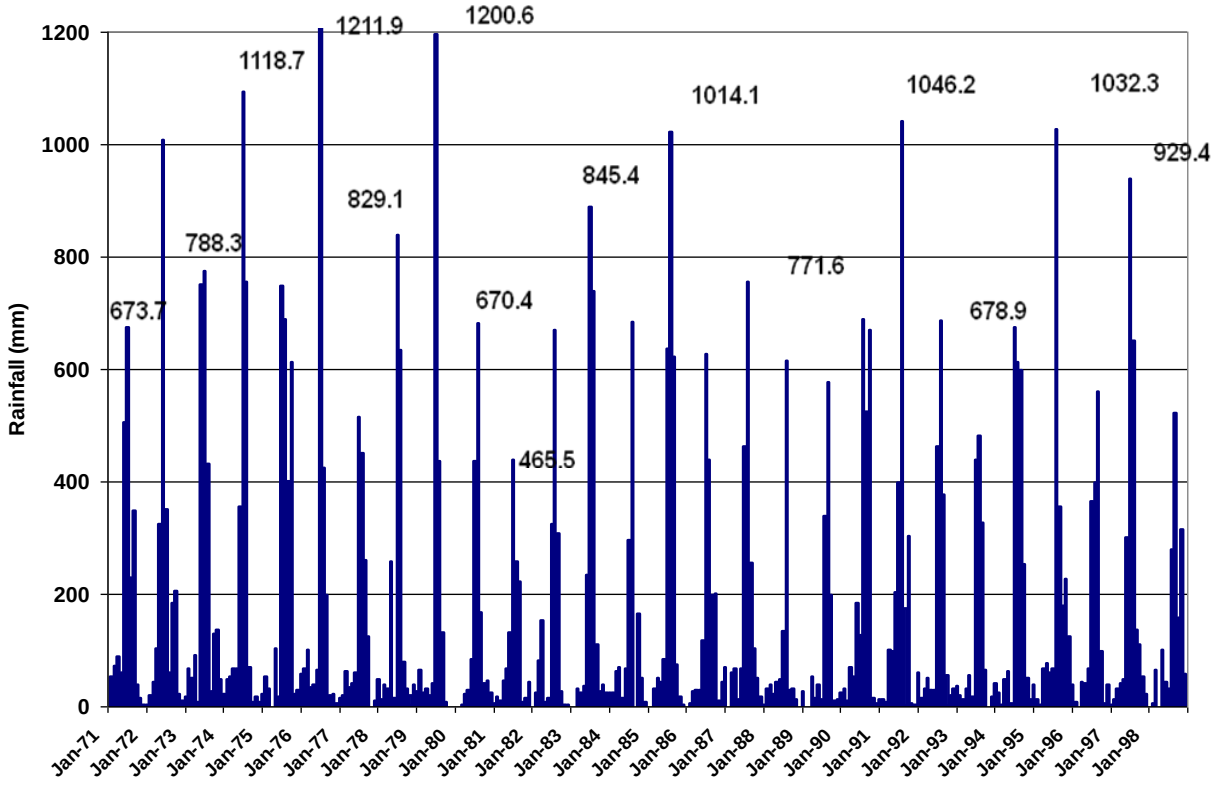

Fig. 5.9 RCM downscaled data (Monthly Rainfall in mm) for the period 2071 to 2098

5.4 Impact of climate change in the study area for various hydrological Scenarios

For the impact of climate change in the Sabari Sub-basin the following three major scenarios has been enumerated for further analysis.

1. Changes in the Runoff if only ET is increased for 10%, 20% and 25%
2. Changes in the Runoff if only Precipitation is increased for 10%, 20% and 25%
3. Changes in the Runoff if both ET and precipitation is increased for 10%, 20% and 25%

All the above scenarios has been developed only for the Mid Century period (2021-2050). Initially ET was calculated for the id century period by incorporating the temperature predicted by the RCM data. The predicted ET and rainfall were used as the input to the ARNO validated model and the runoff was estimated. In this case the peak runoff volume has increased more than 10,000 cumec and this scenario has repeated for few years. Then the intension was to predict the runoff by assuming that the ET has increased to 10%, 20% and 25%. In the first two cases (i.e increase in ET by 10% and 20%) there is in much variations in runoff volume. However, there was a slight decrease in the runoff peaks in the case of increase of ET by 25%.

Like the above case different scenarios was developed and the runoff was estimated with increasing the precipitation by 10%, 20% and 25%. In this case there was slight changes in the runoff volumes if the precipitation is increased by 20 and 25%.

In the third case both the ET and precipitation was increased by 10, 20 and 25% and the runoff were estimated for these three scenarios. In the case of increase of ET and rainfall by 10% the runoff volume has high level of 10,535.67 cumec and this scenario repeated few years. The minimum runoff volume during this scenario was 5841.22 cumec and the average runoff was around 6000 cumec. The plot of this scenario was dicpited in the Fig. 5.10.

In the case of increase of ET and rainfall by 20% the runoff volume has touched the high level of 11,897.35 cumec and this scenario repeated few years. The minimum runoff volume during this scenario was 2356.55 cumec and the average runoff was around 6000 cumec. The plot of this scenario was dicpited in the Fig. 5.11.

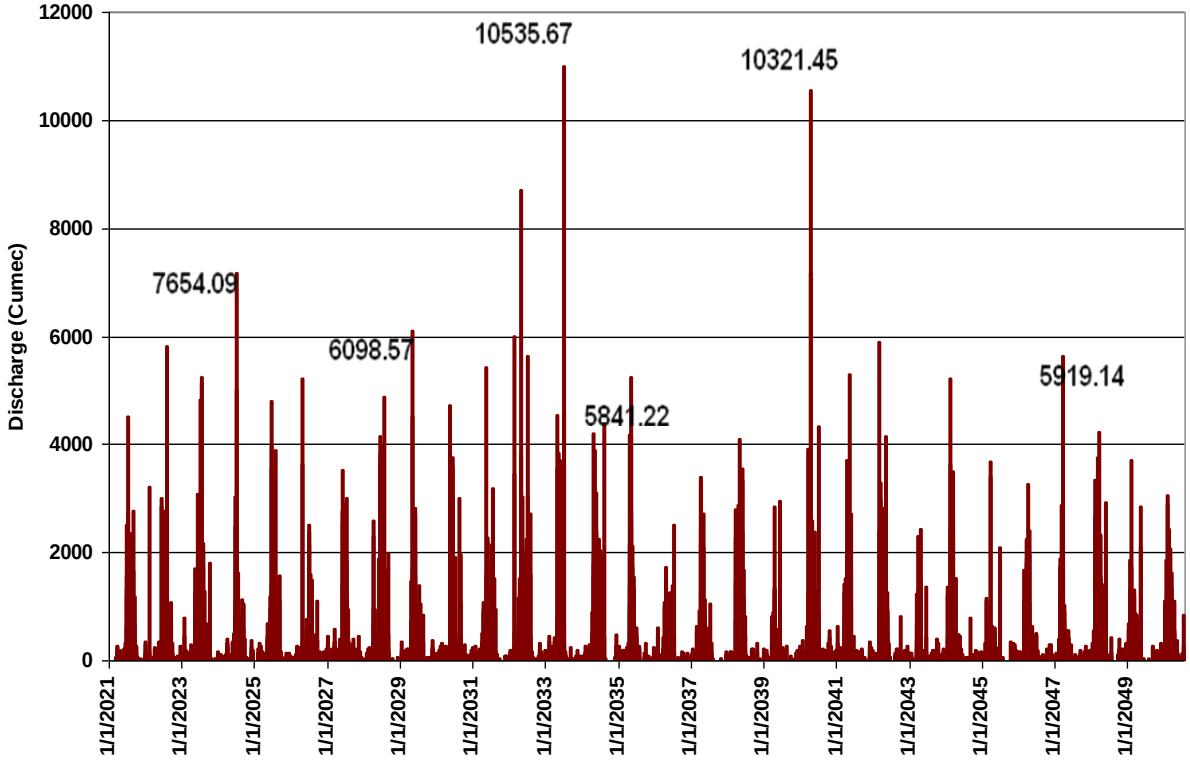

Fig.5.10 Runoff estimation in Sabari Sub-basin if both ET and precipitation is increased for 10%

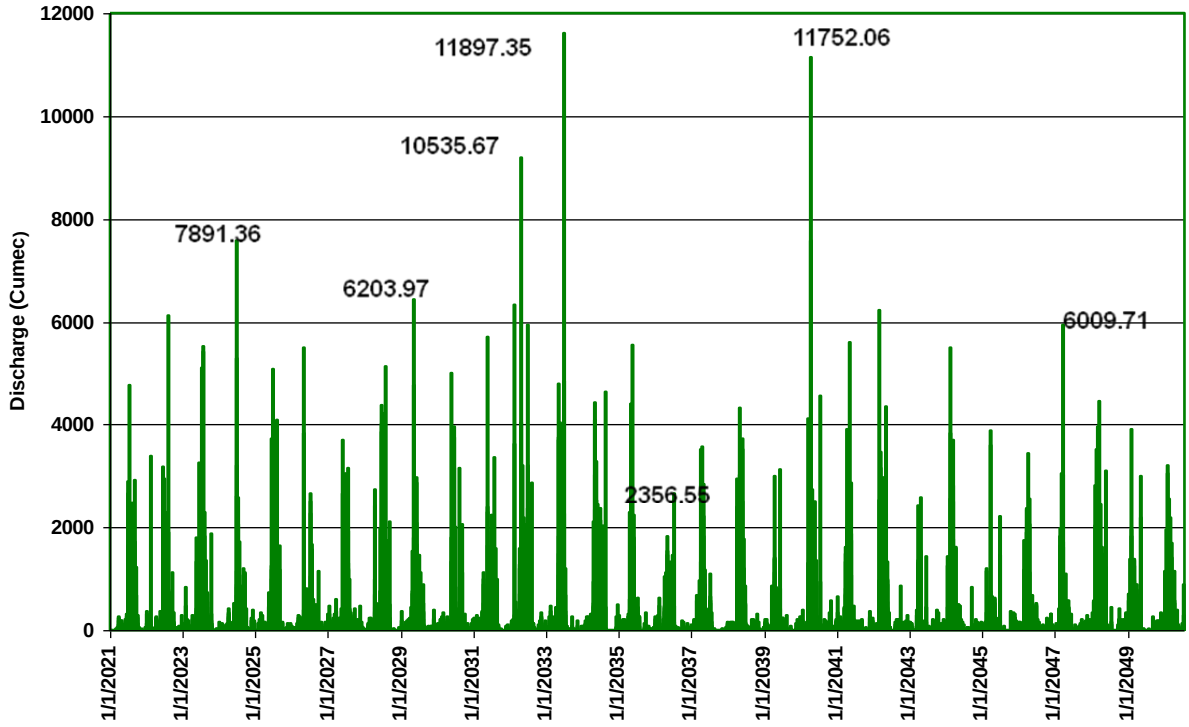

Fig.5.11 Runoff estimation in Sabari Sub-basin if both ET and precipitation is increased for 20%

CHAPTER-6
CONCLUSIONS

Trend analyses of climatic variables (rainfall & temperature) were carried out for Sabari sub-basin using historical period of 109 years (1901 to 2009). Mann-Kendall trend analysis was used to predict the trends of the climatic variables in the study area. The results reveals that the temperature is in increasing trend in the all the months with 95% confidence level. Whereas, rainfall has no trend in monsoon period except the September month shows decreasing trend. Linear trend analysis were also carried out, the results of linear analysis also in line with Mann-Kendall outcome.

The daily rainfall-runoff modeling was carried out using ARNO model for a period of 39 years (1970 to 2008). Calibration and validation was carried out for a period of 30 years (1970 to 1999) and 9 (2000 to 2008) years respectively. The model efficiency during the calibration and validation run was 72.35% and 70.16% respectively.

It is a general practice to use a GCM and determine the futuristic scenarios. The grid size of a GCM model varies from 100 to 250 km. Therefore, GCM is not suitable for the sub-basin scale analysis. Hence, the RCM (Regional Climate Model) data which have a grid cell size of 50 km X 50 km has been used in this study. The RCM data received contains three different scenario periods i.) Base line period (1961 to 1990) ii.) Mid Century Period (2021 to 2050) and iii) End century period (2071 to 2098). The observed IMD and predicted RCM downscaled data for the base line period (1960-1990) has been compared and found that there is a huge variation in both the temperature and rainfall measurements. The temperature is alarmingly increasing during the Mid Century and End Century periods. The futuristic scenarios has been arrived based on the RCM downscaled data. The impact of climate change in the Sabari sub-basin is frequent high peak floods that occurs in a short period of time may alter the landuse/lancover conditions and agricultural patterns in the study area.

References

1. Cannon, J and W. W. Hsieh, 2008. Robust nonlinear canonical correlation analysis: application toseasonal climate forecasting, Nonlin. Processes Geophys., Vol 15, pp 221–232.
2. Droogers,P., A. van Loon, and W. Immerzeel, 2007. Climate change impact assessment as function of model inaccuracy, Hydrol. Earth Syst. Sci. Discuss., Vol 4, pp 2875–2899.
3. Fowler, H.J., C. G. Kilsby, 2007. Using regional climate model data to simulate historical and future river flows in northwest England, spring DOI 10.1007/s10584-006-9117-3, Climatic Change Vol 80, pp337–367.
4. McBean. E and H. Motiee, 2008. Assessment of impact of climate change on water resources:a long term analysis of the Great Lakes of North America, Hydrol. Earth Syst. Sci., Vol 12, pp 239–255.
5. McBean, E and H. Motiee, 2006. Assessment of impacts of climate change on water resources – a case study of the Great Lakes of North America, Hydrology and Earth System Sciences Discussions, Vol.3, pp 3183–3209.
6. Todini, E., Bossi, A., 1986. PAB (Parabolic and Backwater), an unconditionally stable flood routing scheme particularly suited for real time forecasting and control. J. Hydraul. Res., 24(5): 405-424.
7. Todini E., 1988. Il modello afflussi deflussi del fiume Arno. Relazione Generale dello studio per conto della Regione Toscana, Technical Report, Bologna (in Italian).
8. Todini, E., 1996. The ARNO rainfall-runoff model. J Hydrol., 175: 339-382.
9. Todini, E. and Ciarapica L., 2001. The TOPKAPI model in Mathematical Models of Large Watershed Hydrology, Chapter 12, edited by V. P. Singh, D. K. Frevert and S. P. Meyer, Water Resources Publications, Littleton, Colorado, in press.
10. Wang, X. Chen, P. Shi, and P. H. A. J. M. van Gelder, 2008. Detecting changes in extreme precipitation and extreme streamflow in the Dongjiang River Basin in southern China, Hydrol. Earth Syst. Sci., Vol 12, pp 207–221.
11. Xi Chen; Jinglu Wu and Qi Hu, 2008. Simulation of Climate Change Impacts on Streamflow in the Bosten Lake Basin Using an Artificial Neural Network Model,Jjournal of hydrologic engineering, ASCE, DOI: 10.1061/_ASCE_1084-0699_2008_13:3(180).

DIRECTOR: Dr. Raj Dev Singh

COORDINATOR: Dr. Jai Vir Tyagi

HEAD: Dr. Y. R. Satyaji Rao

STUDY GROUP

Dr.V.S.Jeyakanthan, Scientist-D

Dr.Y.R.Satyaji Rao, Scientist-F

B.Krishna, Sc-C